



HAL
open science

Shape-Preserving C^1 GP Hermite Interpolants Generated by a Subdivision Scheme

Francesca Pelosi, Paul Sablonnière

► **To cite this version:**

Francesca Pelosi, Paul Sablonnière. Shape-Preserving C^1 GP Hermite Interpolants Generated by a Subdivision Scheme. *Journal of Computational and Applied Mathematics*, 2008, 220 (1-2), pp.686-711. 10.1016/j.cam.2007.09.013 . hal-00071286

HAL Id: hal-00071286

<https://hal.science/hal-00071286>

Submitted on 23 May 2006

HAL is a multi-disciplinary open access archive for the deposit and dissemination of scientific research documents, whether they are published or not. The documents may come from teaching and research institutions in France or abroad, or from public or private research centers.

L'archive ouverte pluridisciplinaire **HAL**, est destinée au dépôt et à la diffusion de documents scientifiques de niveau recherche, publiés ou non, émanant des établissements d'enseignement et de recherche français ou étrangers, des laboratoires publics ou privés.

Shape-Preserving C^1 GP Hermite Interpolants Generated by a Subdivision Scheme

Francesca Pelosi

*Dipartimento di Scienze Matematiche ed Informatiche, Università di Siena, Pian
dei Mantellini 44, Siena, Italy. E-mail: pelosi@unisi.it*

Paul Sablonnière

*INSA de Rennes, 20 avenue des Buttes de Coësmes, CS 14315, 35043 Rennes
Cedex, France. E-mail: psablonn@insa-rennes.fr*

Abstract

In this paper we present a method for the construction of C^1 Hermite interpolants obtained from a particular family of refinable spline functions introduced by Gori & Pitolli [16]. They constitute a one-parameter subfamily of the Hermite interpolants generated by the general Merrien's subdivision scheme [22]. We compare this family to the other one-parameter subfamily studied by Merrien & Sablonnière [23] and Lyche & Merrien [19] on the solution of two-points Hermite interpolation problems with arbitrary monotonicity or convexity constraints.

Key words: refinable function, interpolation, shape-preservation, corner cutting.

1 Introduction

One of the major research items of approximation theory and of CAGD is the construction of *shape-preserving smooth* interpolants. In this field the literature proposes a huge variety of methods, as for instance C^1 quadratic splines [10,20,29], C^1 cubic splines [2], variable degree polynomials [7,8], parametric splines [21], parametric spline curves [14] and more general schemes [3].

On the other hand, in the last years, subdivision algorithms have been studied and used in many applications, such as wavelets and geometric design.

In order to combine these aspects, we analyze a family of refinable basis functions called *GP B-splines*, introduced by L. Gori and F. Pitolli in [16] and studied in [17,15,18,26]. They generate totally positive bases and possess many interesting properties for CAGD, such as positivity, compact support, partition

of unity, and central symmetry. We focus on the class of *cubic GP B-splines*, which span the space GPS_3 of C^1 *cubic GP splines*. When restricted to a single interval, say $I = [0, 1]$ for the sake of simplicity, they span the local space GPP_3 of *cubic GP polynomials*. We then show that they can be generated by an Hermite subdivision scheme, of the form introduced by Merrien [22,23]. This scheme, that we call $HS(\gamma)$, depends on a parameter $\gamma \in]0, 2[$ which plays the role of a *shape parameter*. Our main purpose is to study the construction of C^1 monotone and/or convex interpolants in GPP_3 , to monotone and/or convex data, by using this Hermite subdivision scheme. We will show that, whatever be the values and the slopes of an increasing or convex function $f \in GPP_3$ at the endpoints of the interval $[0, 1]$, it is *always* possible to construct a C^1 increasing or convex Hermite interpolant to f , by using $HS(\gamma)$. Similar results hold for decreasing or concave functions. Moreover the scheme can be easily generalized to an arbitrary interval $[a, b]$. Since the construction is local, it can be extended to subintervals of an interval endowed with an arbitrary partition, with given values and slopes at the nodes. Therefore is possible to construct C^1 shape-preserving interpolants via simple algorithms. The remaining part of the paper is organized as follows. In Section 2 we briefly recall some basic properties of general GP B-splines, while Section 3 focuses on C^1 cubic GP B-splines. Section 4 is devoted to the construction of the local Bernstein-Bézier representation of cubic GP B-splines: in Subsection 4.1 we first construct a cubic GP Bernstein basis for a single interval, then in Subsection 4.2 we give the description of the associated control net together with a Corner-Cutting Algorithm, and finally Subsection 4.3 presents the main shape-properties of the cubic GP Bernstein basis. In Section 5 we describe the main properties of quadratic GP splines and polynomials. In Section 6, we introduce the family of Hermite subdivision schemes $HS(\gamma)$ depending on a parameter $\gamma \in]0, 2[$, which appears in the two formulas defining the subdivision algorithm. This family includes cubic Hermite interpolants for $\gamma = 1$. It belongs to the family of general subdivision schemes introduced by Merrien. We then prove the C^1 convergence of the algorithm $HS(\gamma)$. While in Section 7, we study a monotone Hermite interpolation problem, we give monotonicity regions and we propose an algorithm for the construction of monotone interpolants to arbitrary non decreasing data $\{y_0, y'_0; y_1, y'_1\}$ by using the subdivision scheme $HS(\gamma)$. In Section 8, we study a convex Hermite interpolation problem, we give convexity regions and we again propose an algorithm for convex interpolants to arbitrary convex data $\{y_0, y'_0; y_1, y'_1\}$ using the subdivision scheme $HS(\gamma)$. In both cases, the algorithms are illustrated by some examples. In all sections, we also compare our subfamily to the subfamily defined in [23] and [19].

2 Definition and properties of GP B-splines

In this section we recall some basic properties of GP B-splines, introduced in [16] and studied in [17,15,18,26]. A GP B-spline of order $m + 1$ can be defined via the following *scaling (or refinement) equation*:

$$\bar{\varphi}_{m+1}(x) = \sum_{k=0}^{m+1} \bar{a}_{k,m+1} \bar{\varphi}_{m+1}(2x - k), \quad (1)$$

where the coefficients depend on a parameter $\gamma \in]0, 2[$

$$\bar{a}_{k,m+1} = \gamma a_{k,m+1} + (1 - \gamma) a_{k-1,m-1}, \quad (2)$$

with $a_{k,m} = \frac{1}{2^{m-1}} \binom{m}{k}$. The *mask* $\bar{\mathbf{a}} = \{\bar{a}_{k,m+1}\}_{k \in \mathbb{Z}}$ satisfies

$$\sum_{k \in \mathbb{Z}} \bar{a}_{2k+1,m+1} = \sum_{k \in \mathbb{Z}} \bar{a}_{2k,m+1} = 1.$$

Moreover the function $\bar{\varphi}_{m+1}$, solution of the refinement equation (1) is positive, compactly supported on $[0, m + 1]$, centrally symmetric, that is

$$\bar{\varphi}_{m+1}(x) = \bar{\varphi}_{m+1}(m + 1 - x), \quad \forall x \in (0, m + 1),$$

and its integer translates form a partition of unity

$$\sum_{k \in \mathbb{Z}} \bar{\varphi}_{m+1}(x - k) = 1, \quad \forall x \in \mathbb{R}.$$

As in [16], it is easy to show that the *symbol* of the mask (2) is a *Hurwitz polynomial* (i.e. a polynomial with roots in the left half plane) for $\gamma \in]0, 2[$. The symbols of the masks of B-splines of degrees $m - 2$ and m being respectively $p_{m-1}(z) = 2^{2-m}(1 + z)^{m-1}$ and $p_{m+1}(z) = 2^{-m}(1 + z)^{m+1}$, the symbol of the GP B-spline with mask $\bar{\mathbf{a}}$ is

$$\begin{aligned} \bar{p}_{m+1}(z) &= 2^{-m}(1 + z)^{m-1} \left(\gamma(1 + z)^2 + 4(1 - \gamma)z \right) \\ &= 2^{-m}((1 + z)^{m-1} \left(\gamma z^2 + 2(2 - \gamma)z + \gamma \right)) \end{aligned}$$

As the discriminant of the quadratic polynomial is $\Delta' = 4(1 - \gamma)$:

- 1) If $0 < \gamma \leq 1$, then $\Delta' \geq 0$ and its roots $z = \gamma - 2 \pm 2\sqrt{1 - \gamma}$ are real and negative.
- 2) If $1 \leq \gamma < 2$, then $\Delta' < 0$ and its roots $z = \gamma - 2 \pm 2i\sqrt{\gamma - 1}$ are complex conjugate.

As \bar{p}_{m+1} has only real negative roots or complex roots with negative real part, it is a Hurwitz polynomial.

Thus $\bar{\varphi}_{m+1}$ is a *ripplelet*, that is $\bar{\varphi}_{m+1}$ is *totally positive*, see [13] for details. As a consequence of this property, the family of integer translates $\{\bar{\varphi}_{m+1}(\cdot - k)\}$ enjoy the variation diminishing properties:

$$S^-(\sum c_j \bar{\varphi}_{m+1}^{(r)}) \leq S^-(\Delta^r c), \quad 0 \leq r \leq m-2 \quad (3)$$

where $S^-(\mathbf{b})$ denotes the number of strict sign changes in the sequence $\mathbf{b} = \{b_j\}_{j \in \mathbb{Z}}$ and $(\Delta^r c)_j = (\Delta^{r-1} c)_{j+1} - (\Delta^{r-1} c)_j$, with $(\Delta^0 c)_j = c_j$.

3 C^1 Cubic GP B-splines

Let us consider the case of *cubic GP B-splines* ($m = 3$) with continuity $C^{m-2} = C^1$ and denote by GPS_3 the space of splines spanned by all combinations of translates of $\bar{\varphi}_4(x)$. From the scale equation,

$$\bar{\varphi}_4(x) = \frac{1}{8} [\gamma \bar{\varphi}_4(2x) + 4\bar{\varphi}_4(2x-1) + (8-2\gamma)\bar{\varphi}_4(2x-2) + 4\bar{\varphi}_4(2x-3) + \gamma \bar{\varphi}_4(2x-4)],$$

we deduce that $\bar{\varphi}_4$ is entirely defined by its values at the 3 points $x = 1, 2, 3$.

Theorem 1 *The values of $\bar{\varphi}_4$ at $x = 1, 2, 3$ are*

$$\bar{\varphi}_4(1) = \bar{\varphi}_4(3) = \frac{\gamma}{2(\gamma+2)} \in \left]0, \frac{1}{4}\right[, \quad \bar{\varphi}_4(2) = \frac{2}{\gamma+2} \in \left]\frac{1}{2}, 1\right[. \quad (4)$$

and the derivatives $D\bar{\varphi}_4$ at the same points are:

$$D\bar{\varphi}_4(1) = \frac{1}{2}, \quad D\bar{\varphi}_4(2) = 0, \quad D\bar{\varphi}_4(3) = -\frac{1}{2}. \quad (5)$$

Proof. From (3), we can compute successively:

$$8\bar{\varphi}_4(1) = \gamma\bar{\varphi}_4(2) + 4\bar{\varphi}_4(1), \quad 8\bar{\varphi}_4(2) = 4\bar{\varphi}_4(3) + (8-2\gamma)\bar{\varphi}_4(2) + 4\bar{\varphi}_4(1).$$

Using the partition of unity and the symmetry w.r.t. $x = 2$, we also have

$$\bar{\varphi}_4(1) + \bar{\varphi}_4(2) + \bar{\varphi}_4(3) = 1.$$

Values (4) are solutions of these equations. With the same kind of technique it is easy to obtain the derivatives (5). \square

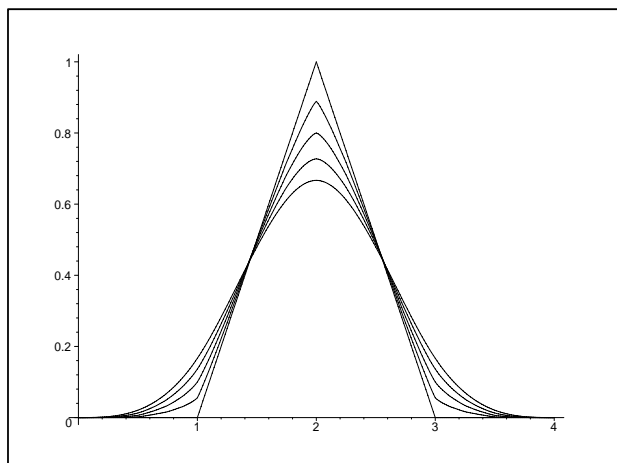


Fig. 1. Example of $\bar{\varphi}_4$ for $\gamma = 0, \frac{1}{4}, \frac{1}{2}, \frac{3}{4}, 1$.

Moreover all values $\{\bar{\varphi}_4(\frac{2k-1}{2}), k = 1, 2, 3, 4\}$ are obtained from the scale equation

$$8\bar{\varphi}_4\left(\frac{2k-1}{2}\right) = \gamma\bar{\varphi}_4(2k-1) + 4\bar{\varphi}_4(2k-2) + (8-2\gamma)\bar{\varphi}_4(2k-3) + 4\bar{\varphi}_4(2k-4) + \gamma\bar{\varphi}_4(2k-5),$$

with, of course, $\bar{\varphi}_4(\ell) = 0$ for $\ell \leq 0$ and $\ell \geq 4$. More generally, all values of $\bar{\varphi}_4$ at the dyadic points of its support can be computed in this way. Some plots of $\bar{\varphi}_4$, for different values of γ , are shown in Figure 1.

4 Bernstein basis and control polygon

4.1 Bernstein basis

The restriction to $I = [0, 1]$ of the space of generalized cubic splines is the space of generalized cubic polynomials

$$GPP_3(I) = \{S(x) = \sum_{j=0}^3 a_j \bar{\varphi}_4(x+j), x \in [0, 1]\},$$

and we can define the corresponding *GP Bernstein basis* $\{b_0, b_1, b_2, b_3\}$. Denoting $e_s(x) = x^s$, we can prove the following

Theorem 2 *There exists a cubic GP Bernstein basis $\{b_0, b_1, b_2, b_3\}$ in the space $GPP_3(I)$ of cubic GP polynomials having the following properties:*

- (1) $b_j(x) \geq 0$ for $x \in [0, 1]$, with $j = 0, 1, 2, 3$;
- (2) $\sum_{j=0}^3 b_j = e_0$;
- (3) $b_j(0) = b_j(1) = 0$, for $j \neq 0, 3$, $b_0(0) = b_3(1) = 1$, and $b_0(1) = b_3(0) = 0$;
- (4) $b'_j(0) = 0$, $j = 2, 3$; and $b'_j(1) = 0$, $j = 0, 1$;
- (5) $b_i(x) = b_{3-i}(1-x)$.

The GP Bernstein basis has the following expression:

$$\begin{aligned}
b_0(x) &= \frac{2(\gamma+2)}{\gamma} \bar{\varphi}_4(x+3), \\
b_1(x) &= \frac{1}{2-\gamma} \left(\frac{\gamma^2-8}{\gamma} \bar{\varphi}_4(x+3) + 2\bar{\varphi}_4(x+2) - \gamma\bar{\varphi}_4(x+1) + 2\bar{\varphi}_4(x) \right), \\
b_2(x) &= \frac{1}{2-\gamma} \left(2\bar{\varphi}_4(x+3) - \gamma\bar{\varphi}_4(x+2) + 2\bar{\varphi}_4(x+1) + \frac{\gamma^2-8}{\gamma} \bar{\varphi}_4(x) \right), \\
b_3(x) &= \frac{2(\gamma+2)}{\gamma} \bar{\varphi}_4(x).
\end{aligned} \tag{6}$$

Proof. From properties (3) and (5), we can set

$$b_0(x) = \frac{2(\gamma+2)}{\gamma} \bar{\varphi}_4(x+3), \quad b_3(x) = b_0(1-x) = \frac{2(\gamma+2)}{\gamma} \bar{\varphi}_4(x),$$

and we define

$$b_1(x) = \pi \bar{\varphi}_4(x+3) + \rho \bar{\varphi}_4(x+2) + \sigma \bar{\varphi}_4(x+1) + \tau \bar{\varphi}_4(x).$$

By symmetry (5), we have

$$b_2(x) = b_1(1-x) = \pi \bar{\varphi}_4(x) + \rho \bar{\varphi}_4(x+1) + \sigma \bar{\varphi}_4(x+2) + \tau \bar{\varphi}_4(x+3).$$

From property (2), we deduce

$$\begin{aligned}
1 &= \left(\frac{2(\gamma+2)}{\gamma} + \pi + \tau \right) \bar{\varphi}_4(x+3) + (\rho + \sigma) \bar{\varphi}_4(x+2) + \\
&\quad (\rho + \sigma) \bar{\varphi}_4(x+1) + \left(\frac{2(\gamma+2)}{\gamma} + \pi + \tau \right) \bar{\varphi}_4(x),
\end{aligned}$$

which gives the two equations

$$\pi + \tau = 1 - \frac{2(\gamma+2)}{\gamma} = -\frac{\gamma+4}{\gamma}, \quad \rho + \sigma = 1.$$

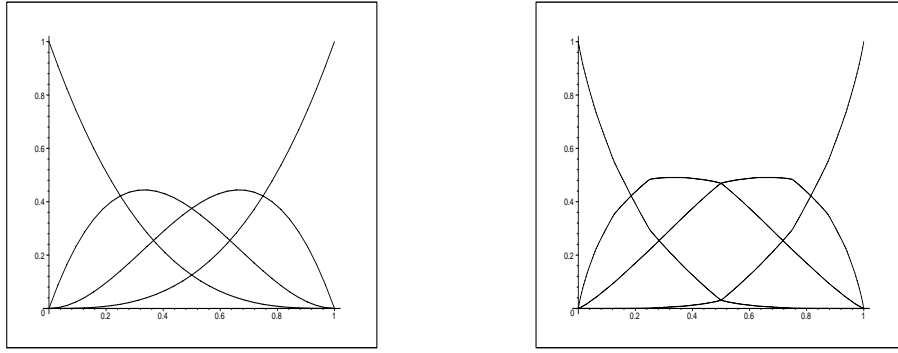


Fig. 2. Examples of cubic GP Bernstein basis in $[0, 1]$ for $\gamma = 1$ (left) and $\gamma = \frac{1}{4}$ (right).

Moreover we have $b'_0(0) = -\frac{\gamma+2}{\gamma}$, and from (3) – (4), $b'_1(0) = -b'_0(0) = \frac{\gamma+2}{\gamma} = \pi\bar{\varphi}'_4(3) + \sigma\bar{\varphi}'_4(1) = \frac{1}{2}(\sigma - \pi)$ and $b_1(1) = 0 = \rho\bar{\varphi}'_4(3) + \sigma\bar{\varphi}'_4(2) + \tau\bar{\varphi}'_4(1)$, which give the two equations:

$$\sigma - \pi = \frac{2(\gamma + 2)}{\gamma}, \quad \gamma\rho + 4\sigma + \gamma\tau = 0.$$

This system of four equations has the following solutions

$$\pi = -\frac{8 - \gamma^2}{\gamma(2 - \gamma)}, \quad \rho = \frac{2}{2 - \gamma}, \quad \sigma = -\frac{\gamma}{2 - \gamma}, \quad \tau = \frac{2}{2 - \gamma}.$$

Therefore we obtain the claim. \square

Figure 2 shows the cubic GP Bernstein polynomials in $[0, 1]$ for the cubic case $\gamma = 1$ and for $\gamma = \frac{1}{4}$. Reciprocally, one obtains the expression of cubic GP B-spline basis in terms of cubic GP Bernstein polynomials.

Theorem 3 For $x \in [i, i + 1]$, the cubic GP B-spline functions are expressed in terms of the local cubic GP Bernstein basis as follows

$$\bar{\varphi}_4(x - i + 3) = \frac{\gamma}{2(\gamma+2)}b_0(x - i), \quad \bar{\varphi}_4(x - i) = \frac{\gamma}{2(\gamma+2)}b_3(x - i),$$

$$\bar{\varphi}_4(x - i + 2) = \frac{1}{\gamma+2} \left(2b_0(x - i) + 2b_1(x - i) + \gamma b_2(x - i) + \frac{\gamma}{2}b_3(x - i) \right).$$

$$\bar{\varphi}_4(x - i + 1) = \frac{1}{\gamma+2} \left(\frac{\gamma}{2}b_0(x - i) + \gamma b_1(x - i) + 2b_2(x - i) + 2b_3(x - i) \right),$$

Proof. For a general subinterval $[i, i + 1]$, we express the B-splines which not vanish as:

| | b_0 | b'_0 | b_1 | b'_1 | b_2 | b'_2 | b_3 | b'_3 |
|-------------------|--------------------|----------------------------|----------------------|---------------------------|----------------------|----------------------------|--------------------|---------------------------|
| $x = 0$ | 1 | $-\frac{\gamma+2}{\gamma}$ | 0 | $\frac{\gamma+2}{\gamma}$ | 0 | 0 | 0 | 0 |
| $x = 1$ | 0 | 0 | 0 | 0 | 0 | $-\frac{\gamma+2}{\gamma}$ | 1 | $\frac{\gamma+2}{\gamma}$ |
| $x = \frac{1}{2}$ | $\frac{\gamma}{8}$ | $-\frac{\gamma+2}{4}$ | $\frac{4-\gamma}{8}$ | $-\frac{\gamma+2}{4}$ | $\frac{4-\gamma}{8}$ | $\frac{\gamma+2}{4}$ | $\frac{\gamma}{8}$ | $\frac{\gamma+2}{4}$ |

Table 1

Values and first derivatives of the cubic GP Bernstein basis at $x = 0, \frac{1}{2}, 1$.

$$\begin{aligned}
\bar{\varphi}_4(x - i + 3) &= \lambda_i b_0(s); \\
\bar{\varphi}_4(x - i + 2) &= \lambda_{i+1} b_0(s) + \mu_{i+1} b_1(s) + \sigma_{i+1} b_2(s) + \nu_{i+1} b_3(s); \\
\bar{\varphi}_4(x - i + 1) &= \lambda_{i+2} b_0(s) + \mu_{i+2} b_1(s) + \sigma_{i+2} b_2(s) + \nu_{i+2} b_3(s); \\
\bar{\varphi}_4(x - i) &= \lambda_{i+3} b_3(s);
\end{aligned}$$

with $s = x - i$. Then we compute λ_i using $\bar{\varphi}_4(3)$ and λ_{i+3} using $\bar{\varphi}_4(1)$. For the expression of $\bar{\varphi}_4(x - i + 2)$ and $\bar{\varphi}_4(x - i + 1)$, we use the expressions of $\bar{\varphi}'_4(3)$ and $\bar{\varphi}'_4(1)$. \square

We collect in Table 1 the values and the first derivatives of the cubic GP Bernstein basis at $x = 0, \frac{1}{2}, 1$, which we will use later.

4.2 Control Polygon and Corner-Cutting Algorithm

From Table 1, we get

$$b'_1(0) = -b'_0(0) = \frac{\gamma + 2}{\gamma}, \quad b'_3(1) = -b'_2(1) = \frac{\gamma + 2}{\gamma},$$

and setting $\theta = \frac{\gamma}{\gamma+2}$, it is easy to verify that

$$e_1 = \theta b_1 + (1 - \theta) b_2 + b_3.$$

This allows to define the control polygon of the (generalized) cubic on $[0, 1]$.

Definition 4 *The control polygon P of*

$$f(x) = a_0 b_0(x) + a_1 b_1(x) + a_2 b_2(x) + a_3 b_3(x),$$

for $x \in [0, 1]$ is the polygonal line connecting the four control vertices $\mathbf{a}_j = (\xi_j, a_j)$, $j = 0, 1, 2, 3$, where

$$\xi_0 = 0, \quad \xi_1 = \theta, \quad \xi_2 = 1 - \theta, \quad \xi_3 = 1.$$

Note that $\theta \in]0, \frac{1}{2}[$ for $\gamma \in]0, 2[$. In particular for $\gamma = 1$, $\theta = \frac{1}{3}$, we obtain the classical cubic control polygon. Figure 3 shows the cubic GP control polygon

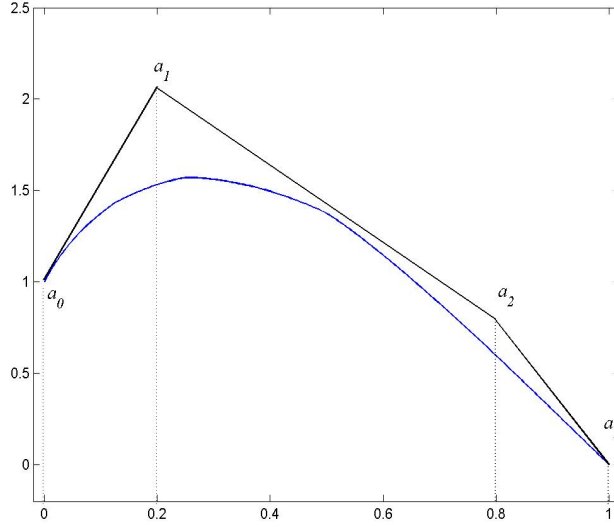


Fig. 3. Control polygon for $\gamma = \frac{1}{2}$.

for $\gamma = 1/2$. Let $f = \sum_{i=0}^3 a_i b_i$, consider now the problem of computing the coefficients of the expansions of f in the Bernstein bases of the two subintervals $I_1 = [0, \frac{1}{2}]$ and $I_2 = [\frac{1}{2}, 1]$ of I . Setting

$$f(t) = f_1(t) = \sum_{i=0}^3 c_i b_i(2t) \quad \text{for } t \in I_1,$$

$$f(t) = f_2(t) = \sum_{i=0}^3 d_i b_i(2t-1) \quad \text{for } t \in I_2,$$

we can prove the following theorem.

Theorem 5 *The coefficients c_j and d_j for $j = 0, 1, 2, 3$ of (7) are computed from the initial coefficients $\{a_j, 0 \leq j \leq 3\}$ by the following formulae*

$$c_0 = a_0, \quad c_1 = \frac{1}{2}(a_0 + a_1) \quad a_4 = \frac{1}{2}(a_1 + a_2), \quad d_2 = \frac{1}{2}(a_2 + a_3), \quad d_3 = a_3,$$

$$c_2 = \frac{\gamma}{2}c_1 + (1 - \frac{\gamma}{2})a_4, \quad d_1 = (1 - \frac{\gamma}{2})a_4 + \frac{\gamma}{2}d_2, \quad c_3 = d_0 = \frac{1}{2}(c_2 + d_1).$$

Proof. By using the values of the GP Bernstein basis at $0, 1/2, 1$ (see Table 1), we immediately obtain the coefficients

$$c_0 = f_1(0) = f(0) = a_0 \quad \text{and} \quad d_3 = f_2(1) = f(1) = a_3,$$

$$c_3 = f_1\left(\frac{1}{2}\right) = d_0 = f_2\left(\frac{1}{2}\right) = f\left(\frac{1}{2}\right) = (a_0 + a_3)\frac{\gamma}{8} + (a_1 + a_2)\frac{4-\gamma}{8},$$

$$f'(0) = \frac{\gamma + 2}{\gamma}(a_1 - a_0) = f'_1(0) = \frac{2(\gamma + 2)}{\gamma}(c_1 - c_0),$$

$$f'(1) = \frac{\gamma + 2}{\gamma}(a_3 - a_2) = f'_1(1) = \frac{2(\gamma + 2)}{\gamma}(d_3 - d_2),$$

whence $c_1 = \frac{1}{2}(a_0 + a_1)$ and $d_2 = \frac{1}{2}(a_2 + a_3)$.

From the equalities $f'(\frac{1}{2}) = f'_1(\frac{1}{2}) = f'_2(\frac{1}{2})$, we obtain the following equation

$$\frac{2}{\gamma}(c_3 - c_2) = -\frac{1}{4}(a_0 - a_3 + a_1 - a_2) = \frac{2}{\gamma}(d_1 - d_0),$$

which gives, after some calculations, the values of c_2 and d_1 . Finally, we have that $c_2 + d_1 = 2c_3 = 2d_0$, whence $c_3 = d_0 = \frac{1}{2}(c_2 + d_1)$. \square

Since $c_3 = d_0 = \gamma(a_0 + a_3)/8 + (4 - \gamma)(a_1 + a_2)/8$, the equalities of Theorem 5, become, in matrix form, the following:

$$[c_0, c_1, c_2, c_3 = d_0, d_1, d_2, d_3]^T = \mathbf{A} [a_0, a_1, a_2, a_3]^T$$

where \mathbf{A} is defined as:

$$\mathbf{A} := \begin{bmatrix} 1 & 0 & 0 & 0 \\ \frac{1}{2} & \frac{1}{2} & 0 & 0 \\ \frac{\gamma}{4} & \frac{1}{2} & \frac{2-\gamma}{4} & 0 \\ \frac{\gamma}{8} & \frac{4-\gamma}{8} & \frac{4-\gamma}{8} & \frac{\gamma}{8} \\ 0 & \frac{2-\gamma}{4} & \frac{1}{2} & \frac{\gamma}{4} \\ 0 & 0 & \frac{1}{2} & \frac{1}{2} \\ 0 & 0 & 0 & 1 \end{bmatrix}. \quad (7)$$

Note that the subdivided polygon defined by $\{c_0, c_1, c_2, c_3=d_0, d_1, d_2, d_3\}$ has been obtained as convex combinations of the polygon defined by $\{a_0, a_1, a_2, a_3\}$. With the intermediate quantity a_4 defined as

$$a_4 = \frac{1}{2}(a_1 + a_2),$$

the subdivision algorithm described in Theorem 5 can be reformulated as follows.

Definition 6 : *Corner-Cutting Algorithm.*

(i) starting with the polygon $\{a_0, a_1, a_2, a_3\}$ we construct $\{c_0, c_1, a_4, d_2, d_3\}$ by cutting the corner in a_1 with the edge (c_1, a_4) and the corner in a_2 with (a_4, d_2) .

(ii) At the second step we construct the polygon $\{c_0, c_1, c_2, d_1, d_2, d_3\}$ by cutting the new corner in a_4 with the edge (c_2, d_1)

$$c_2 = \frac{\gamma}{2}c_1 + (1 - \frac{\gamma}{2})a_4, \quad d_1 = (1 - \frac{\gamma}{2})a_4 + \frac{\gamma}{2}d_2.$$

(iii) At the third step we construct the final control polygon $\{c_0, c_1, c_2, c_3 = d_0, d_1, d_2, d_3\}$ by inserting $c_3 = d_0$ on the edge c_2, d_1 . Since $c_3 = d_0$ and $d_3 = a_3$, the subdivided polygon $\{c_0, c_1, c_2, c_3 = d_0, d_1, d_2, d_3\}$ is obtained by carrying out a corner cutting scheme on $\{a_0, a_1, a_2, a_3\}$.

This scheme can be formulated in matrix form:

$$[c_0, c_1, c_2, c_3 = d_0, d_1, d_2, d_3]^T = \mathbf{S} [a_0, a_1, a_2, a_3]^T$$

where \mathbf{S} is defined as:

$$\mathbf{S} := \begin{bmatrix} 1 & 0 & 0 & 0 & 0 & 0 \\ 0 & 1 & 0 & 0 & 0 & 0 \\ 0 & 0 & 1 & 0 & 0 & 0 \\ 0 & 0 & \frac{1}{2} & \frac{1}{2} & 0 & 0 \\ 0 & 0 & 0 & 1 & 0 & 0 \\ 0 & 0 & 0 & 0 & 1 & 0 \\ 0 & 0 & 0 & 0 & 0 & 1 \end{bmatrix} \begin{bmatrix} 1 & 0 & 0 & 0 & 0 \\ 0 & 1 & 0 & 0 & 0 \\ 0 & \frac{\gamma}{2} & 1 - \frac{\gamma}{2} & 0 & 0 \\ 0 & 0 & 1 - \frac{\gamma}{2} & \frac{\gamma}{2} & 0 \\ 0 & 0 & 0 & 1 & 0 \\ 0 & 0 & 0 & 0 & 1 \end{bmatrix} \begin{bmatrix} 1 & 0 & 0 & 0 \\ \frac{1}{2} & \frac{1}{2} & 0 & 0 \\ 0 & \frac{1}{2} & \frac{1}{2} & 0 \\ 0 & 0 & \frac{1}{2} & \frac{1}{2} \\ 0 & 0 & 0 & 1 \end{bmatrix}. \quad (8)$$

Theorem 7 Assume $0 \leq \gamma \leq 2$, then the matrix \mathbf{S} defined in (8) is totally positive.

Proof. The matrix \mathbf{S} is the product of 3 matrices which are bidiagonal and whose entries are nonnegative for $0 \leq \gamma \leq 2$, thus they are totally positive. Since the product of totally positive matrices is totally positive, we can conclude that also \mathbf{S} is totally positive. \square

4.3 Shape Properties of the cubic GP Bernstein basis

Theorem 8 For $\gamma \in]0, 2[$, the GPP_3 Bernstein basis is totally positive.

The proof follows straightforward the steps of proof for Theorem 11 in [19].

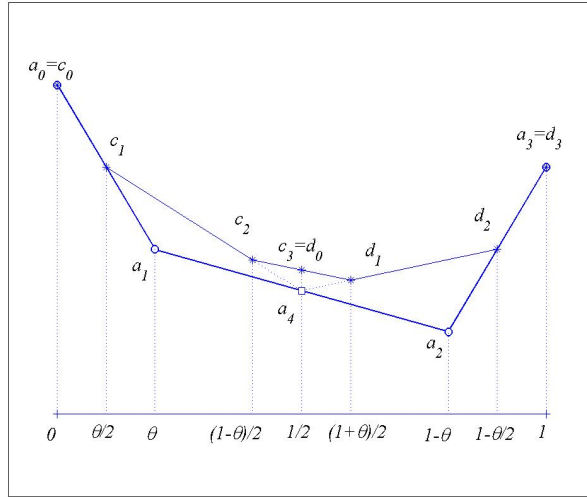


Fig. 4. One step of corner cutting scheme.

Since the GPP_3 Bernstein basis is totally positive, any function $f \in GPP_3(I)$ has the same properties (positivity, convexity and monotonicity) as those of the corresponding control polygon. In particular

Corollary 9 For $\gamma \in]0, 2[$, the Bernstein basis $\{b_0, b_1, b_2, b_3\}$ of GPP_3 has the following properties:

- (1) b_0 is nonnegative, decreasing and convex on $[0, 1]$.
- (2) b_1 is nonnegative and concave on $[0, 1/2]$ and nonnegative, decreasing and convex on $[1/2, 1]$.
- (3) b_2 is nonnegative, increasing and convex on $[1, 1/2]$ and nonnegative and concave on $[1/2, 1]$.
- (4) b_3 is nonnegative, increasing and convex on $[0, 1]$.

Proof. From Theorem 5 and Definition 4 it is immediate to see that the ordinates of the control polygon of the polynomial b_j is the j -th unit vector E_j for $j = 0, 1, 2, 3$. Thus the nonnegativity of b_j follows from the nonnegativity of its control polygon and for the same reason the monotonicity and the convexity properties of b_0 and b_3 hold. For the properties of b_1 and b_2 it suffices to do one subdivision step and to use the relative control polygons: then the proof is similar. \square

5 Quadratic GP splines and polynomials

A similar study can be done for quadratic GP splines and GP polynomials. We denote their spaces respectively by GPS_2 and GPP_2 . As we use the same techniques as in previous sections, we only give the main results in the present one without entering into details. The standard quadratic GP B-spline $\bar{\varphi}_3$ has support $[0, 3]$ and its values are obtained from its refinement equation

$$\bar{\varphi}_3(x) = \frac{1}{4} (\gamma(\bar{\varphi}_3(2x) + \bar{\varphi}_3(2x - 3)) + (4 - \gamma)(\bar{\varphi}_3(2x - 1) + \bar{\varphi}_3(2x - 2))).$$

Moreover, we have $\bar{\varphi}'_4(x) = \bar{\varphi}_3(x) - \bar{\varphi}_3(x - 1)$, therefore if $f = \sum_{i=0}^3 \alpha_i \varphi_4(x + 3 - i)$, for $x \in I$, then we deduce that $f' = \sum_{j=0}^2 \Delta \alpha_j \bar{\varphi}_3(x + 2 - j)$. The symbol $\bar{p}_3(z)$ of $\bar{\varphi}_3$ being a Hurwitz polynomial, the integer translates of this B-spline form a totally positive system having the classical variation diminishing properties. From the above scale equation, we also derive the values of $\bar{\varphi}_3$ at knots and midpoints of its support :

$$\bar{\varphi}_3(1) = \bar{\varphi}_3(2) = 1/2, \quad \bar{\varphi}_3(1/2) = \bar{\varphi}_3(5/2) = \frac{\gamma}{8}, \quad \bar{\varphi}_3(3/2) = 1 - \frac{\gamma}{4}.$$

The Bernstein basis of the local space GPP_2 of quadratic GP polynomials on I is defined by

$$\beta_0(x) = 2\bar{\varphi}_3(x+2), \quad \beta_1(x) = -\bar{\varphi}_3(x+2) + \bar{\varphi}_3(x+1) - \bar{\varphi}_3(x), \quad \beta_2(x) = 2\bar{\varphi}_3(x).$$

Conversely, one has

$$\bar{\varphi}_3(x+2) = \frac{1}{2}\beta_0(x), \quad \bar{\varphi}_3(x+1) = \frac{1}{2}\beta_0(x) + \beta_1(x) + \frac{1}{2}\beta_2(x), \quad \bar{\varphi}_3(x) = \frac{1}{2}\beta_2(x).$$

Therefore, if $g = \sum_{i=0}^2 c_i \beta_i = \sum_{j=0}^2 \gamma_j \varphi_3(x + 2 - j)$, one has

$$c_0 = \frac{1}{2}(\gamma_0 + \gamma_1), \quad c_1 = \gamma_1, \quad c_2 = \frac{1}{2}(\gamma_1 + \gamma_2).$$

and we derive in particular

$$\Delta c_0 = \frac{1}{2}(\Delta \gamma_0), \quad \Delta c_1 = \frac{1}{2}\Delta \gamma_1.$$

This implies that the monotonicity of the sequence of coefficients in the Bernstein basis is equivalent to its monotonicity in the B-spline basis. In particular, when it is nondecreasing, then g is also nondecreasing because of the variation diminishing property of the latter.

One can also express derivatives of the Bernstein basis of GPP_3 in terms of

the Bernstein basis of GPP_2 as follows (we recall that $\theta = \frac{\gamma}{\gamma+2}$):

$$b'_0(x) = -\frac{1}{\theta}\beta_0(x), \quad b'_1(x) = \frac{1}{\theta}\beta_0(x) + \frac{1}{1-2\theta}\beta_1(x),$$

$$b'_2(x) = \frac{1}{1-2\theta}\beta_1(x) - \frac{1}{\theta}\beta_2(x), \quad b'_3(x) = \frac{1}{\theta}\beta_2(x).$$

Therefore, if $f = \sum_{i=0}^3 a_i b_i$, then we obtain

$$f' = \frac{\Delta a_0}{\theta}\beta_0 + \frac{\Delta a_1}{1-2\theta}\beta_0 + \frac{\Delta a_2}{\theta}\beta_2$$

6 Cubic Hermite Subdivision Scheme

In this section we restrict our attention to the interval $I = [0, 1]$ and we consider a cubic GP -polynomial $f(x)$, defined as

$$f(x) = \sum_{i=0}^3 c_i \omega_i(x) \quad (9)$$

where $\omega_i(x) = \bar{\varphi}_4(x - i + 3)$, and satisfying the Hermite interpolation conditions:

$$f(0) = y_0, \quad f(1) = y_1, \quad f'(0) = y'_0, \quad f'(1) = y'_1. \quad (10)$$

The coefficients c_i are obtained by imposing the above conditions,

$$c_0 = \frac{1}{4-\gamma^2} [(\gamma+2)(2y_1 - \gamma y_0) + (\gamma^2 - 8)y'_0 - 2\gamma y'_1],$$

$$c_1 = \frac{1}{4-\gamma^2} [(\gamma+2)(2y_0 - \gamma y_1) + \gamma(2y'_0 + \gamma y'_1)],$$

$$c_2 = \frac{1}{4-\gamma^2} [(\gamma+2)(2y_1 - \gamma y_0) - \gamma(2y'_1 + \gamma y'_0)],$$

$$c_3 = \frac{1}{4-\gamma^2} [(\gamma+2)(2y_0 - \gamma y_1) - (\gamma^2 - 8)y'_1 + 2\gamma y'_0].$$

Let us compute the values of f and f' at $x = 1/2$. By using the values and the first derivatives of the functions ω_i , (4)-(5), we obtain

$$f\left(\frac{1}{2}\right) = \frac{y_0 + y_1}{2} - \frac{\gamma(4-\gamma)}{8(2+\gamma)}(y'_1 - y'_0),$$

$$f' \left(\frac{1}{2} \right) = \frac{\gamma + 2}{2} (y_1 - y_0) - \frac{\gamma}{4} (y_1' + y_0').$$

Therefore we have obtained the initial step of a Merrien subdivision algorithm [23], for the Hermite data (10). Now we consider the general formulation. Suppose that a function f and its first derivative p are given at 0 and 1 and take the values $\{y_0, y_0', y_1, y_1'\}$; f and p are built by induction on the set of dyadic points $D = \cup_n D_n$ where $D_n = \{x = jh, j = 0, \dots, 2^n - 1\}$. At step n , setting $h = 2^{-n}$, then for two consecutive points $a = jh$ and $b = (j + 1)h$ of D_n , f and p are evaluated at the midpoint $m = (a + b)/2$ of $[a, b]$ by the formulas:

$$f(m) = \frac{f(a) + f(b)}{2} + \alpha h(p(b) - p(a)), \tag{11}$$

$$p(m) = (1 - \beta) \frac{f(b) - f(a)}{h} + \beta \frac{p(b) + p(a)}{2},$$

where

$$\alpha = -\frac{\gamma(4 - \gamma)}{8(2 + \gamma)} \quad \text{and} \quad \beta = -\frac{\gamma}{2}. \tag{12}$$

The construction produces an Hermite subdivision scheme $HS(\gamma)$, which depends on the parameter $\gamma \in]0, 2[$: reiterating the process, we define f and p on the set of dyadic numbers $D = \cup_n D_n$, which is dense in $[0, 1]$.

Remark 10 *The above construction shows that an Hermite interpolant in $GPP_3([0, 1])$ can be constructed using Merrien's algorithm with the particular choice (12) of the parameters (α, β) . We call ECS (Extended Cubic Splines), the one parameter family of curves obtained with such values of (α, β) , since it contains the Hermite interpolating cubic polynomials on $[0, 1]$, for $\gamma = 1$, $(\alpha, \beta) = (-\frac{1}{8}, -\frac{1}{2})$.*

Remark 11 *The class of subdivision schemes introduced above belongs to a more general C^1 interpolating subdivision scheme recently studied in [19]. Thus all general results hold for this particular case.*

As in [19], the algorithm can be formulated in a general way. Starting with Hermite data f_0, p_0, f_1, p_1 at the endpoints of a finite interval $[0, 1]$, we set $f_0^0 = f_0, p_0^0 = p_0, f_1^0 = f_1, p_1^0 = p_1$, then for $n = 0, 1, 2, \dots, 2^{-n}$ and $k = 0, 1, \dots, 2^n - 1$

$$f_{2i}^{n+1} := f_i^n, \quad f_{2i+1}^{n+1} := \frac{f_{i+1}^n + f_i^n}{2} + \frac{\alpha}{2^n} (p_{i+1}^n - p_i^n), \tag{13}$$

$$p_{2i}^{n+1} := p_i^n, \quad p_{2i+1}^{n+1} := (1 - \beta) \frac{f_{i+1}^n - f_i^n}{2^n} + \beta \frac{p_{i+1}^n + p_i^n}{2}. \quad (14)$$

Following the same steps of [19], formula (13) can be formulated so that only values of f are involved. Similarly (14) can be formulated only in terms of values of p . We use the notation $\mu = -\frac{\beta}{2}(2 + \beta)$ and $\nu = -\frac{\beta}{2}(1 + \beta)$:

$$\begin{bmatrix} f_{8i}^{n+1} \\ f_{8i+1}^{n+1} \\ f_{8i+2}^{n+1} \\ f_{8i+3}^{n+1} \\ f_{8i+4}^{n+1} \\ f_{8i+5}^{n+1} \\ f_{8i+6}^{n+1} \\ f_{8i+7}^{n+1} \end{bmatrix} = \frac{1}{4} \begin{bmatrix} 4 & 0 & 0 & 0 & 0 \\ 1 + \mu & 2(2 - \mu) & \mu + \nu - 1 & -2\nu & \nu \\ 0 & 4 & 0 & 0 & 0 \\ -\mu & 2(1 + \mu) & 2 - \mu - \nu & 2\nu & -\nu \\ 0 & 0 & 4 & 0 & 0 \\ -\nu & 2\nu & 2 - \mu - \nu & 2(1 + \mu) & -\mu \\ 0 & 0 & 0 & 4 & 0 \\ \nu & -2\nu & \mu + \nu - 1 & 2(2 - \mu) & 1 + \mu \end{bmatrix} \begin{bmatrix} f_{4i}^n \\ f_{4i+1}^n \\ f_{4i+2}^n \\ f_{4i+3}^n \\ f_{4i+4}^n \end{bmatrix}$$

and

$$\begin{bmatrix} p_{4i}^{n+1} \\ p_{4i+1}^{n+1} \\ p_{4i+2}^{n+1} \\ p_{4i+3}^{n+1} \end{bmatrix} = \begin{bmatrix} 1 & 0 & 0 \\ \mu & 1 + \frac{\beta}{2} & -\nu \\ 0 & 1 & 0 \\ -\nu & 1 + \frac{\beta}{2} & \mu \end{bmatrix} \begin{bmatrix} p_{2i}^n \\ p_{2i+1}^n \\ p_{2i+2}^n \end{bmatrix}.$$

Now that f and p have been defined on $D = \cup_{n=0}^{\infty} D_n$, we shall study their continuity on D and also on $[0, 1]$, again the result follows from the general case (see Proposition 4 [19]).

Definition 12 (f, p) is a C^1 interpolant on a set A if f is continuous and admits a first derivative f' with $f' = p$.

Theorem 13 For $\gamma \in]0, 2[$, i.e. $\beta \in]-1, 0[$ and $\alpha \in [\frac{1}{2}(\sqrt{3}-2), 0[$, then (f, p) is a C^1 interpolant on $[0, 1]$.

The minimum value $\bar{\alpha}$ of $\alpha = \frac{\beta(2+\beta)}{4(1-\beta)}$ is attained at $\bar{\beta} = -1 - \sqrt{3}$, and it is equal to $\bar{\alpha} = \alpha(\bar{\beta}) = \frac{1}{2}(\sqrt{3}-2)$. Consider now the matrices $U_n^i \in \mathbb{R}^2$, defined as

$$U_n^i = \begin{bmatrix} p((i+1)2^{-n}) - p(i2^{-n}) \\ \frac{f((i+1)2^{-n}) - f(i2^{-n})}{2^{-n}} - \frac{p((i+1)2^{-n}) - p(i2^{-n})}{2} \end{bmatrix},$$

for $n \in \mathbb{N}$ and $i = 0, \dots, 2^n - 1$. There exist two matrices Λ_1 and Λ_{-1} of $\mathbb{R}^{2 \times 2}$ such that

$$U_{n+1}^{2i} = \Lambda_1 U_n^i, \quad U_{n+1}^{2i+1} = \Lambda_{-1} U_n^i,$$

where

$$\Lambda_\varepsilon = \begin{bmatrix} \frac{1}{2} & \varepsilon(1 - \beta) \\ \varepsilon \frac{8\alpha+1}{4} & \frac{1+\beta}{2} \end{bmatrix}, \quad \varepsilon = \pm 1. \quad (15)$$

In [23] it is shown that if the generalized spectral radius of the set $\Sigma = \{\Lambda_1, \Lambda_{-1}\}$ satisfies $\rho(\Sigma) < 1$, then the function $f' = p$ is Hölder with exponent $-\log_2(\rho)$. An equivalent condition is the existence of a matrix norm $\|\cdot\|$ such that $\|\Lambda_\varepsilon\| < 1, \varepsilon = \pm 1$. In that case, we have $\rho(\Sigma) = \max_{\varepsilon=\pm 1}(\|\Lambda_\varepsilon\|)$.

Since $\alpha = \frac{\beta}{4} \left(\frac{2+\beta}{1-\beta} \right)$, with $\beta \in]-1, 0[$, the matrices (15) can be rewritten in the following form

$$\Lambda_\varepsilon = \begin{bmatrix} \frac{1}{2} & \varepsilon(1 - \beta) \\ \varepsilon \frac{(1+\beta)(1+2\beta)}{4(1-\beta)} & \frac{1+\beta}{2} \end{bmatrix}, \quad \varepsilon = \pm 1. \quad (16)$$

For $\gamma = 1$, i.e. $\beta = -\frac{1}{2}$ and $\alpha = -\frac{1}{8}$ (cubic splines), we have $\rho(\Lambda_\varepsilon) = \frac{1}{2}$. For the general case, we first compute $\det(\Lambda_\varepsilon) = -\frac{1}{2}\beta(1 + \beta)$, then the characteristic polynomial $P(\lambda) = \det(\Lambda_\varepsilon - \lambda I)$ is given by

$$P(\lambda) = \lambda^2 - \frac{1}{2}(2 + \beta)\lambda - \frac{1}{2}\beta(1 + \beta), \quad (17)$$

the roots of which are respectively

$$\lambda_1 = 1 + \beta, \quad \lambda_2 = -\frac{1}{2}\beta.$$

For $\beta \in [-\frac{1}{2}, 0[$, we have $\lambda_1 \geq \lambda_2$, hence $\rho(\{\Lambda_1, \Lambda_{-1}\}) \geq 1 + \beta$. Now we prove that $\rho(\{\Lambda_1, \Lambda_{-1}\}) \leq 1 + \beta$. Consider, for a positive real number θ , the norm defined in \mathbb{R}^2 by $\|(x, y)\|_\theta = |x| + \theta|y|$ and the associated matrix norm in $\mathbb{R}^{2 \times 2}$ defined by $\|M\|_\theta = \max\{|m_{11}| + \theta|m_{21}|, |m_{12}|/\theta + |m_{22}|\}$. By choosing $\theta = \frac{2(1-\beta)}{\beta+1}$, we get $\|\Lambda_{-1}\|_\theta = \|\Lambda_1\|_\theta = 1 + \beta$, thus $\rho(\{\Lambda_1, \Lambda_{-1}\}) \leq 1 + \beta$.

For $\beta \in]-1, -\frac{1}{2}[$, we have $\lambda_2 > \lambda_1$, then we get $\|\Lambda_{-1}\|_\theta = -\beta$ and $\|\Lambda_1\|_\theta = 1 + \beta$, thus $\rho(\{\Lambda_1, \Lambda_{-1}\}) = -\beta$. Both results prove the following

Proposition 14 For $\gamma \in]0, 2[$, i.e. $\beta \in]-1, 0[$, then the function $p = f'$ is Hölder with exponent $\omega(\beta) = -\log_2(1 + \beta)$ for $\beta \in [-\frac{1}{2}, 0[$ and $\omega(\beta) = -\log_2(-\beta)$ for $\beta \in]-1, -\frac{1}{2}]$. Therefore

$$|f'(x) - f'(y)| \leq C|x - y|^{\omega(\beta)}, \quad x, y \in [0, 1].$$

Now we can express a function $f \in GPP_3(I)$, defined from the Hermite interpolation scheme (12), in terms of the GP Bernstein basis, $f(x) = \sum_{i=0}^3 a_i b_i(x)$. Let P be the polygonal line connecting the four control points (ξ_i, a_i) , as in Definition 4. As a consequence of Theorem 9 in [19], we have the following convergence result.

Theorem 15 Let P_n the control polygon obtained from the control polygon P of a function $f \in GPP_3(I)$ after n steps of repeated corner cutting scheme, as described in Theorem 5. Then

$$\lim_{n \rightarrow \infty} P_n = f.$$

7 Monotone Interpolants

The aim of this section is to construct monotone Hermite C^1 interpolants by subdivision. Using a classical model problem stated in [2], with the data $\{y_0, y'_0, y_1, y'_1\} = \{0, x, 1, y\}$ where $(x, y) \in \mathbb{R}_+^2$, we are looking for a parameter γ ensuring the C^1 -convergence of the algorithm (11) to functions $f, p = f'$ such that $p \geq 0$ on $[0, 1]$.

Definition 16 For $(\alpha, \beta) = (-\frac{\gamma(4-\gamma)}{8(2+\gamma)}, -\frac{\gamma}{2})$ we define the monotonicity region

$$M(\alpha, \beta) = \{(x, y) \in \mathbb{R}_+^2 : p \geq 0\}.$$

For $\sigma > 0$, we define the triangular domain

$$T(\sigma) = \{(x, y) \in \mathbb{R}_+^2 : x + y \leq \sigma\}.$$

For $\eta > 0$, we define the square domain

$$Q(\eta) = [0, \eta]^2.$$

For $\delta > 0$, we define the strip

$$B(\delta) = \{(x, y) \in \mathbb{R}_+^2 : -1/2\delta \leq x - y \leq 1/2\delta\}.$$

Proposition 17 Let P be the control polygon (Definition 4) of a function $f \in GPP_3$ interpolating the data $\{0, x, 1, y\}$. Then P is increasing if and only if the pair (x, y) lies in $T\left(\frac{\beta-1}{\beta}\right) = T\left(\frac{1}{\theta}\right)$.

Proof. Setting $f = \sum_{i=0}^3 a_i b_i$, and imposing the interpolation conditions, we get $a_0 = f(0) = 0$ and $a_3 = f(1) = 1$. Since $f'(0) = x$, $f'(1) = y$, we also get $a_1 = \theta x$ and $a_2 = 1 - \theta y$. Thus the control polygon P is increasing if and only $a_1 \leq a_2$, i.e. $\theta x \leq 1 - \theta y$, which is equivalent to $x + y \leq \frac{1}{\theta}$, i.e. $(x, y) \in T\left(\frac{1}{\theta}\right)$, which completes the proof. \square

Theorem 18 For $\gamma \in]0, 2[$, $\beta = -\frac{\gamma}{2} \in]-1, 0[$, and $\alpha = -\frac{\gamma(4-\gamma)}{8(2+\gamma)} \in [\frac{1}{2}(\sqrt{3} - 2), 0[$, the square region $Q\left(\frac{1}{\theta}\right) = Q\left(\frac{\beta-1}{\beta}\right)$ is included in the monotonicity region $M(\alpha, \beta)$.

Proof. with the Hermite data $\{0, x; 1, y\}$, the ordinates of the control polygon P are

$$a_0 = 0, \quad a_1 = \theta x, \quad a_2 = 1 - \theta y, \quad a_3 = 1,$$

with $\theta = \frac{\gamma}{\gamma+2} = -\frac{\beta}{1-\beta}$. After one step of the Corner-Cutting Algorithm, we obtain

$$\begin{aligned} c_0 = 0, \quad c_1 = \frac{1}{2}\theta x, \quad c_2 = \frac{1}{4}((2-\gamma) + 2\theta x - (2-\gamma)\theta y) \\ d_1 = \frac{1}{4}((2+\gamma) + (2-\gamma)\theta x - 2\theta y), \quad d_2 = 1 - \frac{1}{2}\theta y, \quad d_3 = 1, \\ c_3 = d_0 = \frac{1}{8}(4 + (4-\gamma)\theta(x-y)). \end{aligned}$$

By hypothesis, we have $0 \leq \theta x \leq 1$ and $0 \leq \theta y \leq 1$ since $\frac{\beta-1}{\beta} = \frac{1}{\theta}$. Let us now compute the normalized Hermite data $\{0, X_0; 1, Y_0\}$ (respectively $\{0, X_1; 1, Y_1\}$) at the ends of the left (resp. right) subinterval $I_0 = [0, \frac{1}{2}]$ (resp. $I_1 = [\frac{1}{2}, 1]$). First we observe that c_1, d_2 and $a_4 \in [0, 1]$, therefore also c_2, d_1 and finally $c_3 = d_0 \in [0, 1]$. On I_0 , as $f(\frac{1}{2}) = c_3 > 0$, we divide all the coefficients by c_3 in order to get the right normalization. Then, the vertices of the corresponding normalized polygon P_0 on $[0, 1]$ are the following

$$\{(0, 0), (\theta, \frac{c_1}{c_3}), (1 - \theta, \frac{c_1}{c_3}), (1, 1)\}.$$

Therefore the end point derivatives are respectively

$$X_0 = \frac{c_1}{\theta c_3} \geq 0, \quad Y_0 = \frac{c_3 - c_2}{\theta c_3},$$

and we obtain

$$\theta(X_0 + Y_0) = \frac{c - 1 - c_2 + c_3}{c_3}.$$

As $4(c_2 - c_1) = (2 - \gamma)(1 - \theta y) \geq 0$, we have $\theta(X_0 + Y_0) \leq 1$. Second, as $c_1 \leq c_2$, we have $Y_0 \geq 0$, therefore $\theta(X_0 + Y_0) \geq 0$. We can conclude that the polygon P_0 is non decreasing.

On the right subinterval I_1 , we subtract $d_0 > 0$ from the ordinates in order to

get the zero value at the left endpoint. Then, we divide them by $d_3 - d_1 > 0$ in order to get the value 1 at the right endpoint. Indeed $8(d_3 - d_0) = 4 - (4 - \gamma)\theta(x - y) > 0$ since $\theta(x - y) < \frac{4}{4-\gamma}$ for $\gamma \in]0, 2[$.

Thus, the vertices of the right normalized polygon P_1 on $[0, 1]$ are the following

$$\{(0, 0), \left(\theta, \frac{d_1 - d_0}{d_3 - d_0}\right), \left(1 - \theta, \frac{d_2 - d_0}{d_3 - d_0}\right), (1, 1)\}.$$

Therefore the end point derivatives are respectively

$$X_1 = \frac{d_1 - d_0}{\theta(d_3 - d_0)} \geq 0, \quad Y_1 = \frac{d_3 - d_2}{\theta(d_3 - d_0)},$$

and we obtain

$$\theta(X_1 + Y_1) = \frac{d_3 - d_2 + d_1 - d_0}{d_3 - d_0}.$$

First we have $8(d_1 - d_0) = \gamma(2 - \theta(x + y)) > 0$ and $d_3 - d_2 = \frac{1}{2}\theta y \geq 0$, therefore both θX_1 and θY_1 are non negative. Second, as we have

$$1 - \theta(X_1 + Y_1) = \frac{d_2 - d_1}{d_3 - d_0},$$

and $4(d_2 - d_1) = (2 - \gamma)(1 - \theta x) \geq 0$, we conclude that $0 \leq \theta(X_1 + Y_1) \leq 1$, which proves that P_1 is also non decreasing.

By repeating the corner cutting process, we obtain a sequence of non decreasing control polygons which uniformly converges to the function f . Therefore f is also non decreasing. \square

Figure 5 shows some examples of monotonicity regions for $\beta = -3/8, -1/2, -1/4, -1/8$.

The above theorem defines a square contained in $M(\alpha, \beta)$, in order to give a better localization of the latter, we shall define two regions $\widetilde{M}(\alpha, \beta)$ and $\overline{M}(\alpha, \beta)$ such that:

$$\overline{M}(\alpha, \beta) \subseteq M(\alpha, \beta) \subseteq \widetilde{M}(\alpha, \beta),$$

both containing the square $Q(\frac{\beta-1}{\beta})$. Suppose f is monotone increasing, then $f'(1/2) \geq 0$, which gives:

$$x + y \leq \frac{2(\beta - 1)}{\beta}, \tag{18}$$

thus $M(\alpha, \beta) \subseteq T(2(\beta - 1)/\beta)$, where $T(2(\beta - 1)/\beta)$ is a triangular domain. If we impose the nonnegativity of the derivatives at $1/4, 3/4, 3/8, 5/8$, we obtain the inequalities:

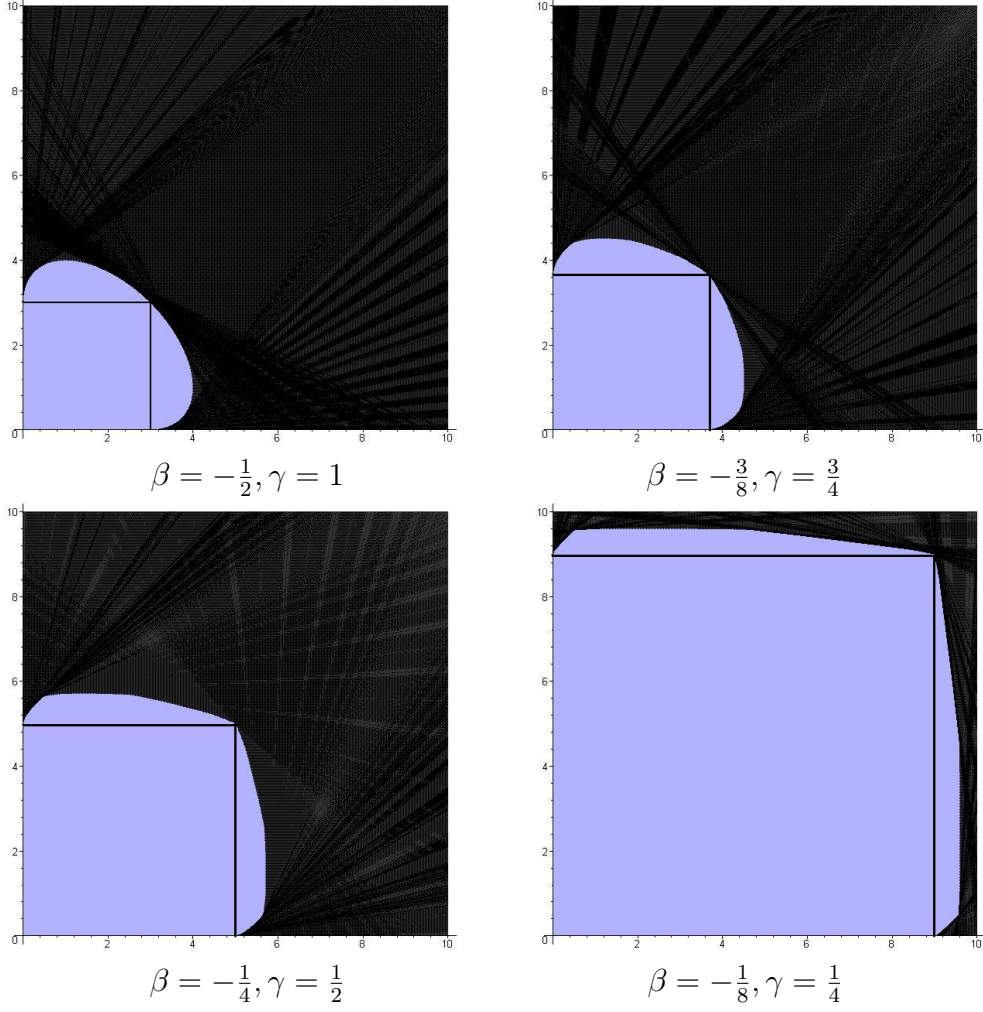


Fig. 5. Some examples of monotonicity regions $M(\alpha, \beta)$, for different values of β together with $Q(\frac{\beta-1}{\beta})$.

$$\begin{aligned}
y &\leq \frac{\beta + 2}{4 + 3\beta} x + \frac{2(\beta + 2)(\beta - 1)}{\beta(4 + 3\beta)}, \\
y &\geq \frac{4 + 3\beta}{\beta + 1} x - \frac{2(\beta + 2)(\beta - 1)}{\beta(\beta + 1)}, \\
y &\leq \frac{(4 + 3\beta)\beta}{(\beta + 2)(\beta + 4)} x + \frac{2(2 - \beta)(\beta - 1)}{\beta(4 + \beta)}, \\
y &\leq \frac{(\beta + 2)(\beta + 4)}{(4 + 3\beta)\beta} x + \frac{2(\beta - 2)(\beta - 1)(\beta + 2)}{\beta^2}.
\end{aligned}$$

The region $\tilde{M}(\alpha, \beta)$ of points satisfying the above inequalities and (18) is delimited by the polygonal line connecting the points $\tilde{A}_1, \tilde{A}_2, \tilde{A}_3, \tilde{A}_4, \tilde{A}_5, \tilde{A}_6$ and $\tilde{A}_0 = (0, 0)$:

$$\begin{aligned}
\tilde{A}_1 &:= \frac{2(\beta-1)}{\beta} \left(0, \frac{2+\beta}{4+3\beta} \right), \\
\tilde{A}_2 &:= \frac{2(\beta-1)(\beta+2)}{\beta(2\beta^3+4\beta^2-\beta-4)} (\beta+1, \beta^2+\beta-1), \\
\tilde{A}_3 &:= \frac{2(\beta-1)}{\beta(2\beta^2+5\beta+4)} ((\beta+1)(\beta+2), \beta^2+2\beta+2), \\
\tilde{A}_4 &:= \frac{2(\beta-1)}{\beta(2\beta^2+5\beta+4)} (\beta^2+2\beta+2, (\beta+1)(\beta+2)), \\
\tilde{A}_5 &:= \frac{2(\beta-1)(\beta+2)}{\beta(2\beta^3+4\beta^2-\beta-4)} (\beta^2+\beta-1, \beta+1), \\
\tilde{A}_6 &:= \frac{2(\beta-1)}{\beta} \left(\frac{2+\beta}{4+3\beta}, 0 \right).
\end{aligned}$$

Now, we define the region $\overline{M}(\alpha, \beta)$ included in $M(\alpha, \beta)$ that contains the square $Q(\frac{\beta-1}{\beta})$. Using theorem 4, we first observe that the control polygon obtained after one step of the corner-cutting algorithm is non decreasing if and only if the following conditions are satisfied on the first control polygon :

$$a_0 \leq \min(a_1, a_2) \quad \text{and} \quad \max(a_1, a_2) \leq a_3.$$

From the values $a_0 = 0, a_1 = \theta x, a_2 = 1 - \theta y, a_3 = 1$, we deduce that for $\theta x \leq 1 - \theta y$, the above conditions are automatically satisfied. For $\theta x \geq 1 - \theta y$, we must have both x and $y \leq \frac{1}{\theta}$, i.e. exactly the condition of theorem 9 : $(x, y) \in Q(\frac{1}{\theta})$. Now, we will find conditions on the data (x, y) in order that the control polygon obtained after 2 steps of the corner-cutting algorithm be nondecreasing. Using the notations of section 4.2, the following conditions must be satisfied in each of the two subpolygons obtained after the first step of the corner-cutting algorithm

$$c_0 \leq \min(c_1, c_2) \quad \text{and} \quad \max(c_1, c_2) \leq c_3, \quad d_0 \leq \min(d_1, d_2) \quad \text{and} \quad \max(d_1, d_2) \leq d_3.$$

Writing these conditions, we obtain the four inequalities :

$$\begin{aligned}
y &\leq \frac{x}{1+\beta} + \frac{\beta-1}{\beta}, & y &\geq (1+\beta)x - \frac{\beta^2-1}{\beta}, \\
y &\leq \frac{\beta}{\beta+2}x + \frac{2(\beta-1)}{\beta(\beta+2)}, & y &\geq \frac{\beta+2}{\beta}x + \frac{2(1-\beta)}{\beta^2}.
\end{aligned}$$

We denote respectively $\overline{D}_1, \overline{D}_4, \overline{D}_2, \overline{D}_3$ the straight lines associated with the corresponding equalities, delimiting the polygonal region $\overline{M}(\alpha, \beta)$. We have certainly $\overline{M} \subset M$ because the control polygon being nondecreasing at the second step, the convergence of the corner-cutting algorithm implies the monotonicity of the limit curve. The vertices of the hexagon \overline{M} are the points

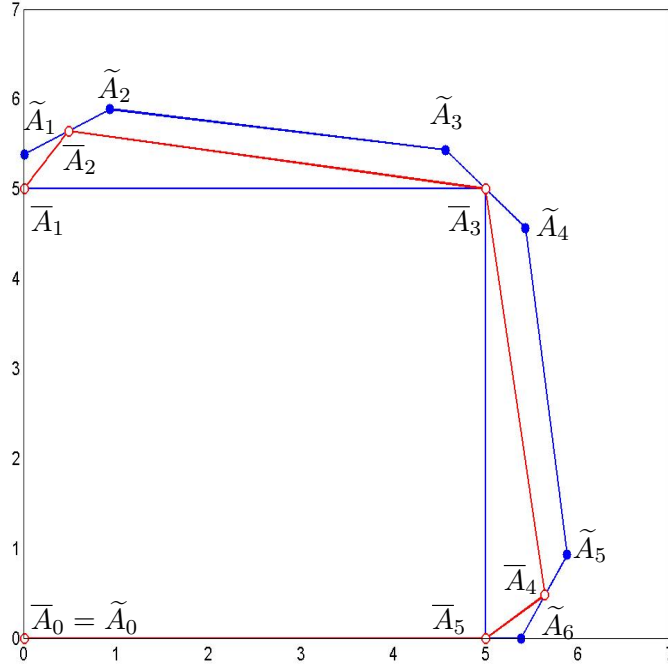


Fig. 6. Examples of the regions $Q((\beta - 1)/\beta)$, $\bar{M}(\alpha, \beta)$ and $\tilde{M}(\alpha, \beta)$, for $\beta = -1/4$.

$\bar{A}_i, 0 \leq i \leq 5$, with

$$\bar{A}_0 = (0, 0), \bar{A}_1 = \left(0, \frac{\beta - 1}{\beta}\right), \bar{A}_2 = \left(\frac{1 - \beta^2}{2 - \beta^2}, \frac{(\beta - 1)^2(\beta + 2)}{\beta(\beta^2 - 2)}\right), \bar{A}_3 = \left(\frac{\beta - 1}{\beta}, \frac{\beta - 1}{\beta}\right),$$

the two points \bar{A}_4 and \bar{A}_5 being symmetric points of \bar{A}_2 and \bar{A}_1 respectively, with respect to the line $y = x$. Figure 6 shows the regions $\bar{M}(\alpha, \beta)$ and $\tilde{M}(\alpha, \beta)$.

Remark 19 From proposition 2, we deduce that the monotonicity region $T\left(\frac{\beta-1}{\beta}\right)$ of the control polygon does not coincide with $Q\left(\frac{\beta-1}{\beta}\right)$. Thus the monotonicity of the control polygon implies the monotonicity of the function, but in general the converse is not true.

Remark 20 We notice that, for $\gamma \rightarrow 0$, $\beta \rightarrow 0^-$ and $\lim_{\beta \rightarrow 0^-} \frac{\beta-1}{\beta} = +\infty$, So the square region $Q\left(\frac{\beta-1}{\beta}\right)$ dilates up to the whole plane as β tends to zero. From Theorem 18, we can conclude that, for limit values of β or γ , there exists a monotone interpolant for each data pair (x, y) .

Remark 21 By analyzing the asymptotic behavior of the straight lines bounding the regions \tilde{M} and \bar{M} , we notice that the distances between \tilde{M} and \bar{M} and between M and \bar{M} tend to zero when $\beta \rightarrow 0$.

7.1 Algorithms for Monotone Interpolants

We assume that the interpolant is monotone increasing with boundary data

$$\{y_0, y'_0; y_1, y'_1\} = \{0, x; 1, y\},$$

where $(x, y) \in \mathbb{R}_+^2$. The construction is similar for the decreasing case.

The first algorithm is based on the inclusion $Q(\frac{\beta-1}{\beta}) \subset M(\alpha, \beta)$.

First we choose a *parameter* $\lambda \geq 1$, which can be used as shape parameter in order to force the point (x, y) to lie inside the monotonicity region, and we set $\eta = \lambda \max\{x, y\}$.

Case 1: $0 \leq \eta \leq 3$. Since $\max\{x, y\} = \frac{\eta}{\lambda}$ we have $(x, y) \in Q(\frac{\eta}{\lambda})$, where $Q(\frac{\eta}{\lambda}) \subset Q(3)$, and so by choosing $\beta = -\frac{1}{2}$, we can interpolate by *classical cubic splines*.

Case 2: $\eta > 3$. We can choose $\beta = \frac{1}{1-\eta}$, thus we have $\eta = \frac{\beta-1}{\beta}$ and $-\frac{1}{2} < \beta < 0$. As a consequence of Theorem 18:

$$(x, y) \in Q\left(\frac{\eta}{\lambda}\right) \subset Q(\eta) \subset M(\alpha, \beta),$$

therefore the corresponding interpolant is increasing.

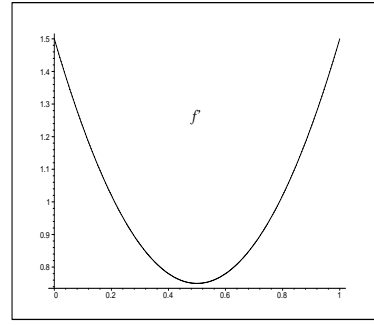
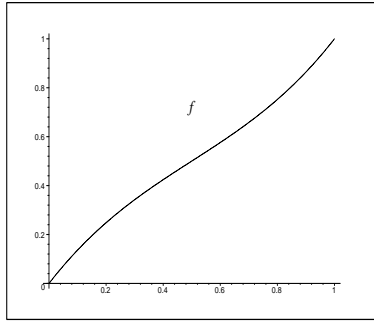
Figure 8 shows some monotone interpolants together with the relative first derivatives. These pictures have to be compared with those obtained in [23] and reported in Figure 7.

The algorithm for monotone interpolants can be improved by using the inclusion $\overline{M}(\alpha, \beta) \subset M(\alpha, \beta)$.

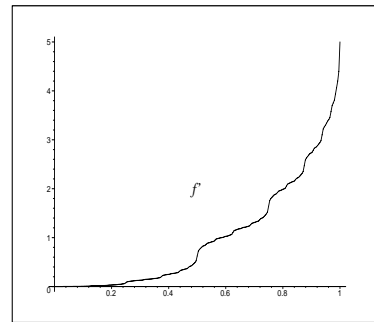
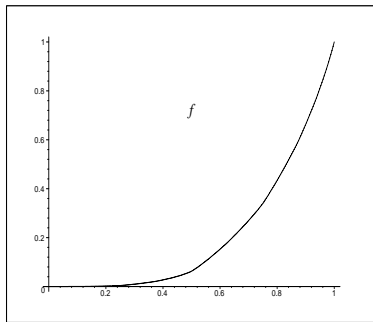
7.2 Comparison of Merrien's monotone interpolants

Let *EQS* (extended quadratic splines) be the family of interpolants defined in [23], with $\alpha = \frac{\beta}{4(1-\beta)}$ and let *ECS* (extended cubic splines) the family of interpolants studied in this paper, with $\alpha = \frac{\beta(\beta+2)}{4(1-\beta)}$. We want here to compare the smoothness of derivatives of the *EQS* and the *ECS* both for monotone and convex interpolants. When $f \in EQS$, then its derivative f' is Hölder with exponent $\omega_1(\beta') = -\log_2(1 + \beta')$, where $\beta' = \frac{1}{2}\beta$. When $f \in ECS$, then its derivative f' is Hölder with exponent $\omega_2(\beta) = -\log_2(1 + \beta)$ (Proposition 1, Section 6).

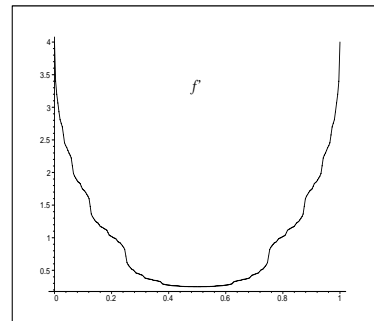
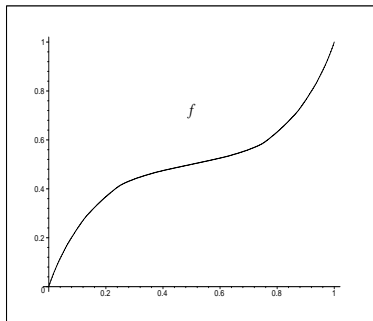
For the case of monotone interpolants, we consider a given pair (x, y) of posi-



$$x = 1.5, y = 1.5, \beta = -\frac{1}{2}, \gamma = 1$$



$$x = 0, y = 5, \beta = -\frac{1}{4}, \gamma = \frac{1}{2}$$

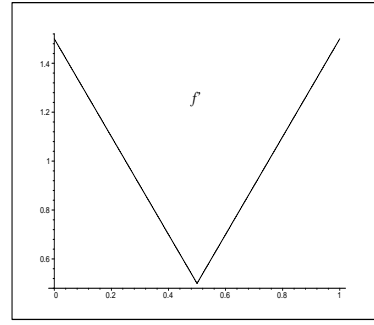
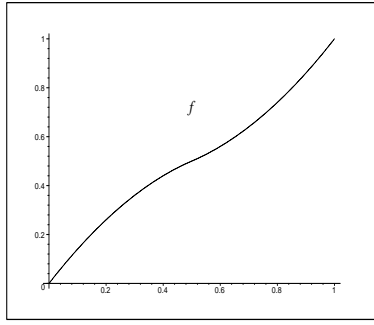


$$x = 4, y = 4, \beta = -\frac{1}{4}, \gamma = \frac{1}{2}$$

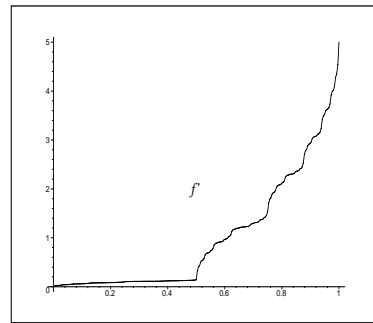
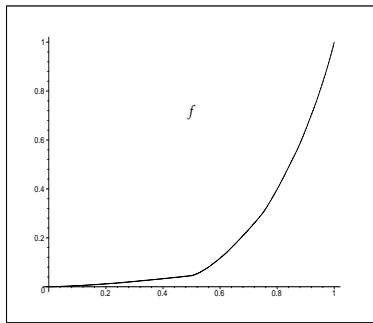
Fig. 7. Examples of monotone interpolants with $HS(\gamma)$.

tive derivatives at the end points, we take $\lambda = 1$ for the sake of simplicity. Then $f \in EQS$ is nondecreasing if $\beta'_1 = -\frac{1}{(x+y-2)}$ and $f \in ECS$ is nondecreasing if $\beta_2 = -\frac{1}{(\max(x,y)-1)}$.

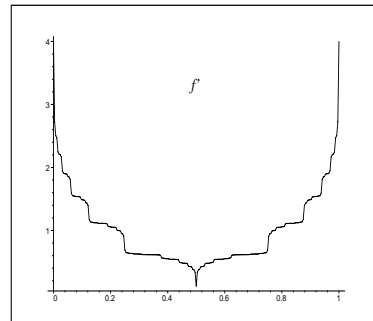
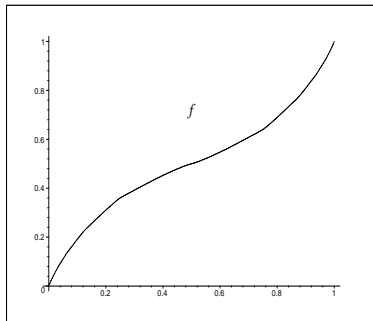
It turns out that $f \in ECS$ is smoother than $f \in EQS$ when x and y have close values. The converse is true when x and y have quite distinct values.



$$x = 1.5, y = 1.5, \beta = -1,$$



$$x = 0, y = 5, \beta = -0.57143$$



$$x = 4, y = 4, \beta = -0.29412$$

Fig. 8. Examples of monotone interpolants obtained in [23].

Let consider the following examples.

Example 1 : for $(x, y) = (4, 4)$, then we consider $\beta_1 = -\frac{1}{6}$ for f_1 and $\beta_2 = -\frac{1}{3}$ for f_2 . In that case, f_1 is smoother than f_2 .

Example 2 : for $(x, y) = (5, 0)$, then we consider $\beta_1 = -\frac{1}{3}$ for f_1 and $\beta_2 = -\frac{1}{4}$ for f_2 . In that case, f_1 is smoother than f_2 .

However, when $x \geq \frac{1}{2}$ (or $y \geq \frac{1}{2}$), the result can be slightly improved by considering the larger polygonal region included in the monotonicity region defined in Section 6.

Example 3 : for $(x, y) = (5, 0.5)$, then we consider $\beta_1 = -\frac{2}{7} \approx -0.286$ for $f_1 \in EQS$ and $\beta_2 = -\frac{1}{4}$ for $f_2 \in ECS$, hence f_1 is smoother than f_2 . However, if we choose $\beta = \beta'_2 = -0.3$, then the point (x, y) lies in the monotonicity region, for it satisfies the two inequalities

$$-\frac{2+\beta}{\beta}x + y \leq \frac{2(1-\beta)}{\beta^2} \quad \text{and} \quad (1+\beta)x - y \leq \frac{\beta^2 - 1}{\beta}$$

Therefore we have got an interpolant $f_2 \in ECS$ which is smoother than $f_1 \in EQS$.

8 Convex Interpolants

In this section, we build convex Hermite C^1 interpolants, by using the model problem associated with the boundary data $\{y_0, y'_0, y_1, y'_1\} = \{0, -x, 0, y\}$, where $(x, y) \in \mathbb{R}_+^{*2}$ ($x > 0$ and $y > 0$). We are looking for a parameter γ ensuring the C^1 -convergence of the algorithm (11) to the functions $f, p = f'$ such that p is increasing on $[0, 1]$.

Definition 22 For $(\alpha, \beta) = (-\frac{\gamma(4-\gamma)}{8(2+\gamma)}, -\frac{\gamma}{2})$ we define the convexity cone

$$C(\alpha, \beta) = \{(x, y) \in \mathbb{R}_+^{*2} : p \text{ increasing}\}.$$

For $\eta > 0$, we define the cone domain

$$C^*(\eta) = \{(x, y) \in \mathbb{R}_+^{*2} : 1/\eta \leq y/x \leq \eta\}.$$

Proposition 23 Let P be the control polygon (as in Definition 4) of a GPP_3 function f interpolating the data $\{0, -x; 0, y\}$. Then P is convex if and only if $(x, y) \in C^*(1/|\beta|)$.

Proof. Setting $f = \sum_{i=0}^3 a_i b_i$, then the interpolation conditions give $a_0 = a_3 = 0$, $a_1 = -\theta x$ and $a_2 = -\theta y$. Thus the control polygon P is convex if and only if:

$$\begin{aligned} \frac{a_1 - a_0}{\theta} \leq \frac{a_2 - a_1}{1 - 2\theta} \leq \frac{a_3 - a_1}{\theta} &\Leftrightarrow -x \leq \frac{\theta}{1 - 2\theta}(x - y) \leq y \\ &\Leftrightarrow |\beta|x \leq y \leq \frac{1}{|\beta|x} \Leftrightarrow (x, y) \in C^*\left(\frac{1}{|\beta|}\right). \end{aligned}$$

□

From the convergence result expressed in Theorem 15 and as consequence of the proposition above, we have the following.

Theorem 24 For $\gamma \in]0, 2[$, $\beta \in]-1, 0[$, then f is convex if and only if its control polygon is convex, i.e.

$$C^*(1/|\beta|) = C(\alpha, \beta).$$

Proof. First, assume that the control polygon P is convex, i.e. $(x, y) \in C^*(\frac{1}{|\beta|})$ or $2x - \gamma y \geq 0$ and $2y - \gamma x \geq 0$. Using the results of Section 5, we deduce that $f' = -x\beta_0 - \frac{\theta}{1-2\theta}(y-x)\beta_1 + y\beta_2$. This function is nondecreasing because the inequalities

$$-x \leq -\frac{\theta}{1-2\theta}(y-x) \leq y$$

are equivalent to

$$\theta y \leq (1-\theta x) \quad \text{and} \quad \theta x \leq (1-\theta y),$$

which are themselves equivalent to the convexity of P . Therefore, as f' is nondecreasing, f is convex.

Now, we assume that f is convex and we shall prove that its initial control polygon P is also convex. We assume that $f = \sum_{i=0}^3 a_i b_i$ is convex and we have to prove that its initial control polygon P is also convex. As $f' = \frac{\Delta a_0}{\theta} \beta_0 + \frac{\Delta a_1}{1-2\theta} \beta_1 + \frac{\Delta a_2}{\theta} \beta_2$, it suffices to prove that when $g = \sum_{i=0}^2 c_i \beta_i \in GPP_2$ is nondecreasing, then the sequence (c_0, c_1, c_2) of its B-coefficients is also nondecreasing (i.e. the converse of the variation diminishing property seen in section 5). For example, one can prove that if this sequence is convex and nonincreasing, then g is nonincreasing.

Without loss of generality, we can choose $w_0 = [c_0, c_1, c_2]^T = [0, -\omega, 1]^T$ where $\omega > 0$ is an arbitrary small parameter. The problem is to find some value of g which is negative by applying the corner-cutting (CC-)algorithm in GPP_2 . It is easy to prove that the first step of this algorithm gives the following sequence of B-coefficients (d_0, d_1, d_2) on the left subinterval $[0, 1/2]$:

$$d_0 = c_0, \quad d_1 = \frac{\gamma}{2}c_0 + \overline{M} \left(1 - \frac{\gamma}{2}\right) c_1, \quad g(1/2) = d_2 = \frac{\gamma}{4}c_0 + \overline{M} \left(1 - \frac{\gamma}{2}\right) c_1 + \frac{\gamma}{4}c_2.$$

Defining the matrix

$$A = \begin{bmatrix} 1 & 0 & 0 \\ \frac{\gamma}{2} & 1 - \frac{\gamma}{2} & 0 \\ \frac{\gamma}{4} & 1 - \frac{\gamma}{2} & \frac{\gamma}{4} \end{bmatrix},$$

we see that $w_1 = [d_0, d_1, d_2]^T = Aw_0$. Continuing this process, we obtain the sequence of vectors w_n of B-coefficients of g in the first subinterval $[0, 1/2^n]$ of the n -th step of the CC-algorithm. The eigenvalues and eigenvectors of A are respectively:

$$\lambda_1 = 1, v_1 = [1, 1, 1]^T; \lambda_2 = 1 - \frac{\gamma}{2}, v_2 = [0, 1 - \frac{3}{4}\gamma, 1 - \frac{\gamma}{2}]^T; \lambda_3 = \frac{\gamma}{4}, v_3 = [0, 0, 1]^T$$

Let P be the matrix having v_1, v_2, v_3 as column vectors, then $A = PDP^{-1}$ where

$$D = \begin{bmatrix} 1 & 0 & 0 \\ 0 & 1 - \frac{1}{2}\gamma & 0 \\ 0 & 0 & \frac{1}{4}\gamma \end{bmatrix},$$

then $w_n = A^n w_0 = PD^n P^{-1} w_0$. The vector $v_0 = P^{-1} w_0 = [x_0, y_0, z_0]^T$ is solution of the system $Pv_0 = w_0$, and we obtain

$$x_0 = 0, y_0 = -\frac{4\omega}{4 - 3\gamma}, z_0 = 1 + 2\omega \frac{2 - \gamma}{4 - 3\gamma},$$

from which we deduce $w_n = (\xi_n, \eta_n, \zeta_n)^T$, with $\zeta_n = g(2^{-n})$ given by

$$\zeta_n = -2\omega \frac{2 - \gamma}{4 - 3\gamma} \left[\left(1 - \frac{1}{2}\gamma\right)^n - \left(\frac{1}{4}\gamma\right)^n \right] + \left(\frac{1}{4}\gamma\right)^n.$$

As we want $\zeta_n < 0$, we must have

$$\left(\frac{4}{\gamma}\right)^n \zeta_n = -2\omega \frac{2 - \gamma}{4 - 3\gamma} \left[\left(\frac{2}{\gamma}\right)^n (2 - \gamma)^n - 1 \right] + 1 < 0.$$

As $\left(\frac{2}{\gamma}\right)^n (2 - \gamma)^n \rightarrow +\infty$ when $n \rightarrow +\infty$, it is clear that there exists an index n large enough such that this inequality is true. In particular, we get $g(1/2) < 0$. \square

Figure 9 shows some examples of convexity regions for $\beta = -3/8, -1/2, -1/4, -1/8$.

8.1 Algorithm for Convex Interpolants

We assume that the interpolant is convex with boundary data $\{y_0, y'_0, y_1, y'_1\} = \{0, -x, 0, y\}$ and $(x, y) \in \mathbb{R}_+^2$. The construction is similar for the concave case.

First suppose $y/x \geq 1$, we choose a *parameter* $\lambda \geq 1$, which can be used as shape parameter in order to force the point (x, y) to lie inside the convexity region and we set $\gamma = \lambda y/x$, thus:

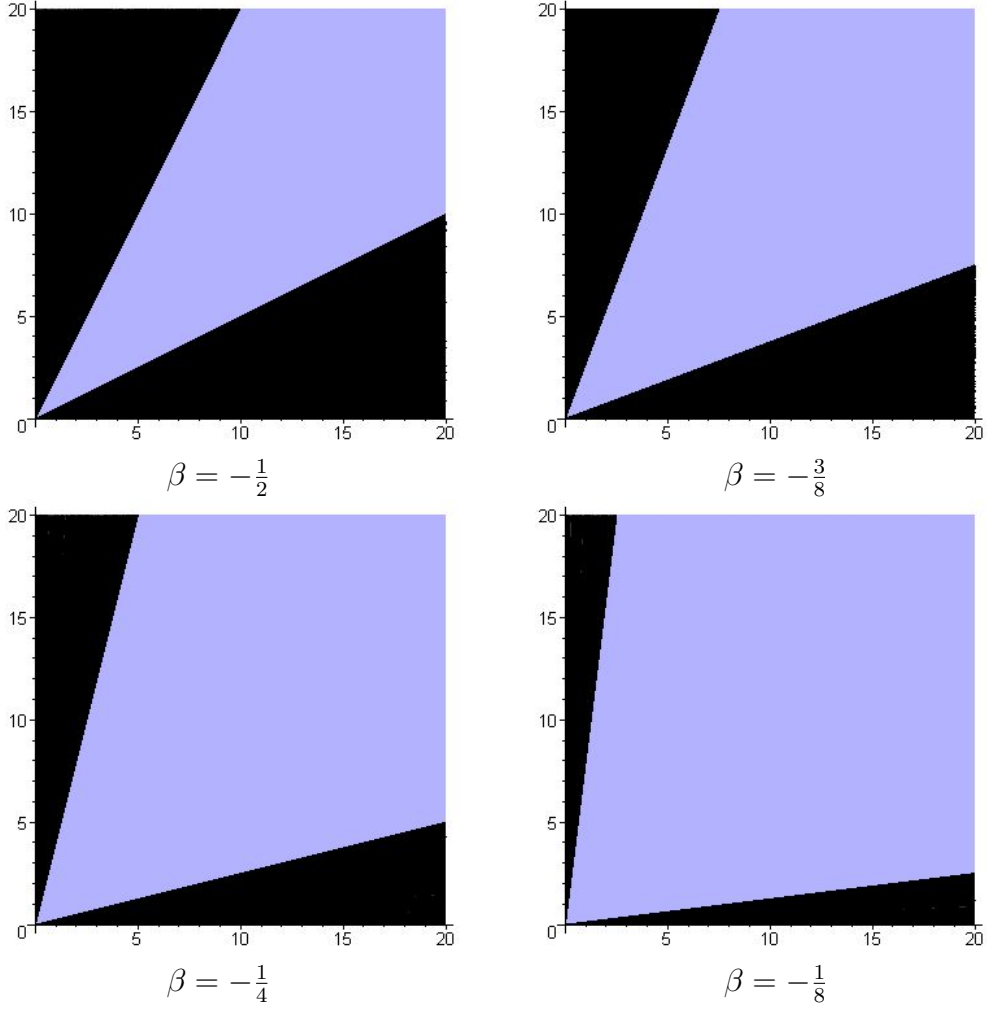


Fig. 9. Some examples of convexity regions for different values of β .

Case 1: $1 \leq \eta \leq 2$. Since $y/x = \frac{\eta}{\lambda}$ then $(x, y) \in C^*(\frac{\eta}{\lambda}) \subset C(2)$, and so by choosing $\beta = -\frac{1}{2}$, we can interpolate by cubic splines.

Case 2: $\eta > 2$. We can choose:

$$\beta = -\frac{1}{\eta},$$

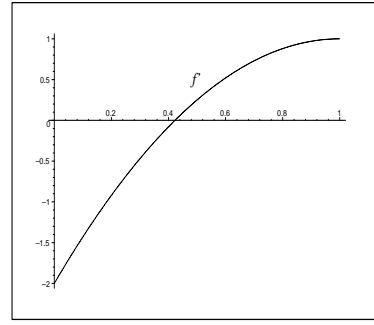
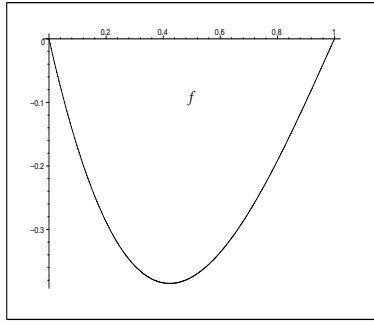
we have $\eta = \frac{1}{|\beta|}$ and $-\frac{1}{2} \leq \beta \leq 0$, and as consequence of Theorem 24, we have:

$$(x, y) \in C^*\left(\frac{\eta}{\lambda}\right) \subset C^*(\eta) \subset C(\alpha, \beta),$$

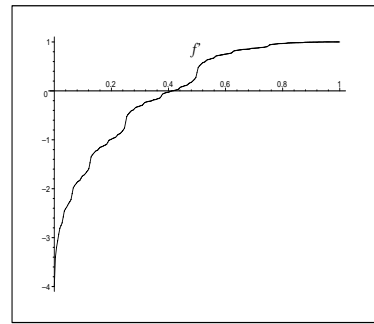
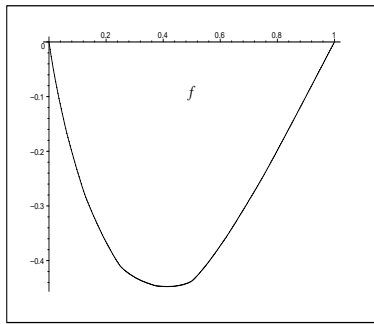
therefore the corresponding interpolant is convex.

Now suppose $y/x \leq 1$, we choose a *parameter* $\lambda \geq 1$ and we set $\gamma = \lambda x/y$, thus:

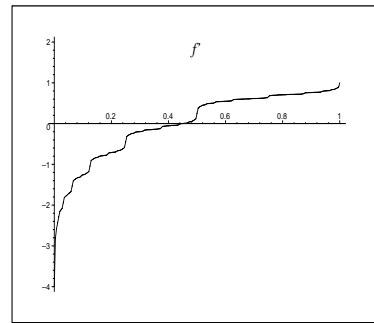
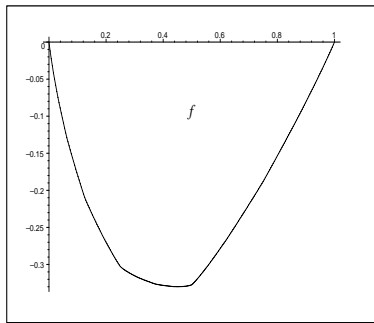
Case 1': $1 \leq \eta \leq 2$. Since $y/x = \frac{\lambda}{\eta}$ then $(x, y) \in C^*(\frac{\eta}{\lambda}) \subset C(2)$, by choosing $\beta = -\frac{1}{2}$, we can interpolate by cubic splines.



$$x = 2, y = 1, \beta = -\frac{1}{2}, \gamma = 1$$



$$x = 4, y = 1, \beta = -\frac{1}{4}, \gamma = \frac{1}{2}$$



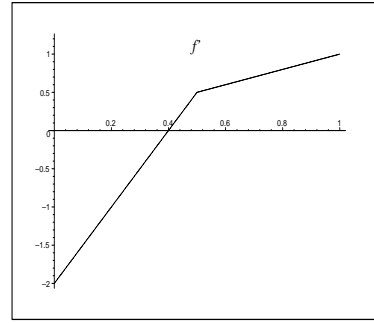
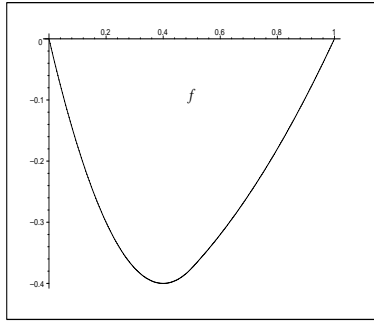
$$x = 4, y = 1, \beta = -\frac{1}{6}, \gamma = \frac{1}{3}$$

Fig. 10. Examples of convex interpolants with $HS(\gamma)$.

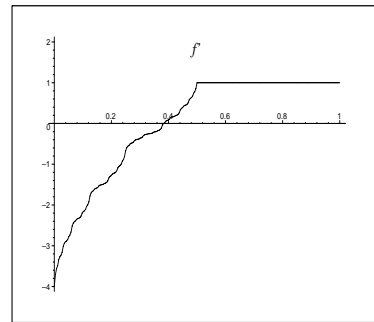
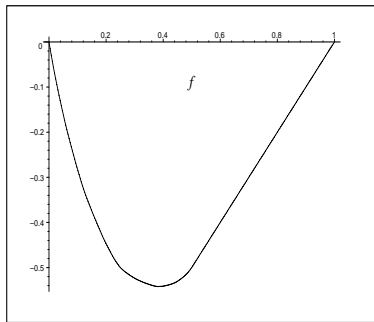
Case 2': $\eta > 2$. We can choose:

$$\beta = -\frac{1}{\eta},$$

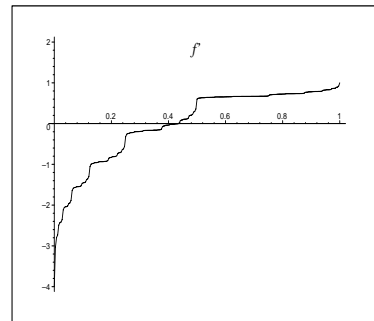
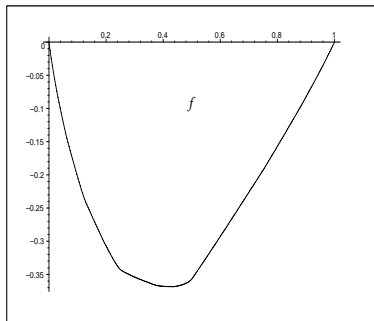
as in Case 2.



$$x = 2, y = 1, \beta = -\frac{1}{2}, \gamma = 1$$



$$x = 4, y = 1, \beta = -\frac{1}{4}, \gamma = \frac{1}{2}$$



$$x = 1, y = 2, \beta = -\frac{1}{6}, \gamma = \frac{1}{3}$$

Fig. 11. Examples of convex interpolants obtained in [23].

Figure 10 shows some convex interpolants together with the relative first derivatives. Again, these pictures have to be compared with those obtained in [23] and reported in Figure 11.

8.2 Comparison of Merrien's convex interpolants

For the case of convex interpolants, we assume that $y < x$ and we set $\eta = \frac{x}{y}$, with $\lambda = 1$. For $f \in EQS$ and $\eta > 3$, then the convexity region is $C_1 = C^*(\gamma) = C^*(\frac{\beta-2}{\beta})$. Therefore we obtain $\beta = -\frac{2}{\gamma-1}$, i.e. $\beta_1 = -\frac{1}{\gamma-1}$. For $f \in ECS$ and $\eta > 2$, then the convexity region is $C_2 = C^*(\gamma) = C^*(\frac{1}{|\beta|})$. Therefore we obtain $\beta_2 = -\frac{1}{\gamma} > \beta_1$. This shows that $f \in EQS$ is always smoother than $f \in ECS$. However, for large values of γ , as $\beta_2 - \beta_1 = \frac{1}{\gamma(\gamma-1)}$, the two values of β_1 and β_2 are quite close to each other.

References

- [1] C. de Boor, *A practical guide to splines*. (revised edition). Springer-Verlag, New-York, 2001.
- [2] R.E. Carlson and F.N. Fritsch, Monotone piecewise cubic interpolation. *SIAM J. Numer. Anal.*, **17** (1980), 230–246.
- [3] J. Carnicer and W. Dahmen, Characterization of local strict convexity preserving interpolation by C^1 functions, *J. Approx. Theory*, **77**, (1994) 2–30.
- [4] J. Carnicer and J.M. Peña, Totally positive bases for shape preserving curves design and optimality of B-splines. *Comput. Aided Geom. Design* **11** (1994) 633-654.
- [5] J. Carnicer and J.M. Peña, Total positivity and optimal bases. In *Total Positivity and its Applications*, M. Gasca, C.A. Micchelli (eds), Kluwer, Dordrecht 1996, 133-155.
- [6] A. Cavaretta, W. Dahmen, C.A. Micchelli, Stationary subdivision. *Mem. Amer. math. Soc.*; **93**, 1991.
- [7] P. Costantini, On monotone and convex interpolation, *Math. Comp.*, **46**, (1986) 203–214.
- [8] P. Costantini, Co-monotone interpolating splines of arbitrary degree. A local approach, *SIAM J. Sci. Statist. Comput.*, **8**, (1986) 1026–1034.
- [9] R. Delbourgo and J.A. Gregory, Piecewise rational quadratic interpolation to monotonic data, *IMA J. Numer. Anal.*, **2**, (1982) 123–130.
- [10] R. DeVore and G.G Lorentz, *Constructive Approximation*, Springer-Verlag, Berlin, (1993).
- [11] N. Dyn, D. Levin, Subdivision schemes. In *Acta Numerica 2002*, A. Iserles (ed), Cambridge University Press, **11**(2002), 73–144.

- [12] Edelman A. and Micchelli C., Admissible slopes for monotone and convex interpolation by parametrically defined curves., *Numer. Math.*, **51**, (1987) 441–458.
- [13] T.N.T. Goodman, C.A. Micchelli : On refinement equations determined by Polya frequency sequences. *SIAM J. Math. Anal.* **23** (1992) 766-784.
- [14] T.N.T. Goodman and K. Unsworth, Shape-preserving interpolation by parametrically defined curves, *J. Approx. Theory, SIAM J. Numer. Anal.*, **25**, (1988) 1453–1465.
- [15] L. Gori, L. Pezza and F. Pitolli, A class of totally positive blending B-Bases, in: Laurent P.J., Sablonnière P., Schumaker L.L. (eds.), *Curve and Surfaces Design*, Saint Malo, 1999, Vanderbilt University Press, Nashville, TN, (1999), 119–126.
- [16] L. Gori and F. Pitolli, Multiresolution analysis based on certain compactly supported refinable functions, *Proceeding of ICAOR: International Conference on Approximation and Optimization (Romania)*, (G. Coman, W.W. Breckner, P. Blaga, eds.), Transilvania Press, (1997), 81–90.
- [17] L. Gori and F. Pitolli, A class of totally positive refinable functions, *Rend. Mat. Ser. VII* **20**, (2000) 305–322.
- [18] L. Gori, F. Pitolli and E. Santi, Positive Refinable Operators, *Numer. Algorithms* **28**, (2001) 199–213.
- [19] T. Lyche, J.L. Merrien, C^1 interpolatory subdivision schemes with shape constraints. *Prépublication IRMAR 04-61*, Université de Rennes, December 2004.
- [20] D.F. MacAllister and J.A. Roulier, Interpolation by convex quadratic splines, *Math. Comp.*, **32**, (1987) 1154–1162.
- [21] C. Manni, C^1 comonotone Hermite interpolation via parametric cubics, *J. Comp. Appl. Math.*, **2**, (1992) 187–200.
- [22] J.L. Merrien, A family of Hermite interpolants by bisection algorithms, *Numer. Algor.*, **69**, (1996) 143–157.
- [23] J.L. Merrien and P. Sablonnière, Monotone and convex C^1 Hermite interpolants generated by subdivision scheme, *Constr. Approx.*, **29** (2003) 279–298.
- [24] C.A. Micchelli, *Mathematical aspects of geometric modeling*. CBMS-NSF Regional Conference Series in Applied Mathematics. SIAM, Philadelphia, 1995.
- [25] C.A. Micchelli, H. Prautzsch, Refinement and subdivision for spaces of integer translates of a compactly supported function. In *Numerical Analysis 1987*, R. Griffith, G. Watson (eds), Longman, Harlow, 1988, 192-222.

- [26] F. Pitolli, Refinement masks of Hurwitz type in the cardinal interpolation problem, *Rend. Mat. Ser. VII* 18, (1998) 473–487.
- [27] P. Sablonnière, Bernstein-type bases and corner-cutting algorithms for C^1 Merrien’s curves, *Adv. Comput. Math.*, **20**, (2004) 229–246.
- [28] L.L. Schumaker, *Spline functions : basic theory*. John Wiley & Sons, New-York 1981.
- [29] L.L. Schumaker, On shape preserving quadratic spline interpolation, *SIAM J. Numer. Anal.* **20**, (1983) 854–864.